UAlg FCT
UNIVERSIDADE DO ALGARVE
FACULDADE DE CIÊNCIAS E TECNOLOGIA

Universidade do Algarve

Optimal light wavelength and intensity for algae cultivation in photobioreactors

Gustavo Filipe Magalhães Nogueira

Dissertação

Mestrado em Aquacultura

Trabalho efetuado sob a orientação de:

Dr. Peter Simon Claus Schulze

&

Prof. Dr. João Carlos Serafim Varela

2024

Universidade do Algarve
Faculdade de Ciências e Tecnologia

Optimal light wavelength and intensity for algae cultivation in photobioreactors

by

Gustavo Filipe Magalhães Nogueira

Supervised by

Dr. Peter Simon Claus Schulze

Associação Oceano Verde – GreenCoLab, Faro, Portugal

&

Prof. Dr. João Carlos Serafim Varela

Universidade do Algarve, Faro, Portugal

performed at

Faculdade de Ciências e Tecnologias,
Universidade do Algarve, Portugal
Faro, Portugal

Associação Oceano Verde – GreenCoLab,
Universidade do Algarve,
Faro, Portugal

2024

Declaração de autoria de trabalho

Declaro ser o autor deste trabalho, que é original e inédito. Autores de trabalhos consultados estão devidamente citados no texto e constam de listagem de referências incluídas.

_____	_____	_____
Gustavo Nogueira	Location	Date

Acknowledgments

First and foremost, I would like to express my deepest gratitude to my supervisors, Dr. Peter Simon Claus Schulze from Associação Oceano Verde (GreenCoLab), and Prof. Dr. João Varela from the University of Algarve (UAlg), Centre of Marine Science (CCMar), for their unwavering support and encouragement throughout the completion of this thesis, as well as for their critical review and feedback. Special thanks again to Dr. Peter Schulze for never giving me direct answers, encouraging me to explore solutions independently, and helping me build confidence in my problem-solving abilities through trial and error. His guidance has not only shaped me as a researcher but also as an independent thinker. I would also like to dedicate the development of the AlgaeLum light system to him. Also, I would like to thank Gabriel Bombo, Culture Collection Manager from GreenCoLab, for his invaluable assistance and mentorship, ranging from daily lab activities to hands-on practical work, without which I would never have been able to design and construct the efficient experimental setups used in this study. Furthermore, I would like to thank Dr. Hugo Pereira, General Manager from GreenCoLab, for allowing me to conduct my experiments in GreenCoLab's facilities and for providing opportunities to connect with many talented professionals. My heartfelt thanks go out to the entire team at GreenCoLab for helping me overcome the many challenges I encountered during this study. Last but not least, I want to give a very special thanks to my whole family for their acceptance and their aid to my studying abroad.

Abstract

In the present study, the growth response of *Phaeodactylum tricornutum*, *Nannochloropsis oceanica*, and *Porphyra dioica cultures* with different biomass concentrations to 22 combinations of red (620 nm), green (530 nm), and blue (450 nm) light at 3 different light intensities (200, 500, and 1000 μmol m^{-2} s^{-1}) was investigated. Photosynthetic oxygen evolution rates as response variable were used to create predictive models with the optimal light conditions to improve growth at different algal growth stages. While *P. dioica* did not result in positive oxygen evolution rates and thus no model could be established, for *P. tricornutum* and *N. oceanica,* predictive models showed statistical significance and were used to develop light regimes, matching the needs of algae cultures at different growth stages (lag, exponential, and late exponential phase). The generated models predicted the least absorbed wavelength (620 nm) as optimal for both algae, suggesting that it penetrated the algal culture deeper and stimulated photosynthesis of more cells than more absorbed wavelengths (e.g., 450 nm) that do not penetrate deeper into the culture. An additional experiment was conducted to validate the obtained light regimes. For this purpose, a novel light system (AlgaeLum) was developed, 3D printed and assembled for testing different light quantities and qualities. Experiments showed no significant differences in growth rate and maximum biomass concentrations compared to the control warm white light for both algae. Less absorbed wavelengths showed to improve photosynthetic efficiency in both microalgal species, especially in highly dense cultures and low light paths, over highly absorbed wavelengths (450 nm). Based on this result, the use of red light (620 nm) LEDs is recommended for *N. oceanica* and *P. tricornutum* as it offers an optimal balance between cost-effectiveness in terms of both CAPEX and OPEX) and photosynthetic efficiency. The developed AlgaeLum system can be used in the future to conduct other trials (e.g., continuous cultivation systems), which was not tested in the present study to validate the present results.

Keywords:

Microalgae, Photobioreactor, Light Wavelengths, Light Intensity, Photosynthesis

Resumo

O produto final derivado do cultivo das microalgas é utilizado na alimentação humana, ração animal, cosméticos, produção de biocombustíveis, tratamento de águas residuais, biotecnologia e farmacêutica, além de também ser utilizado na agricultura como biofertilizantes e bioestimulantes. Isto resulta do facto da biomassa de microalgas ser rica em componentes de valor acrescentado, como proteínas, ácidos gordos polinsaturados, vitaminas, polissacáridos, e pigmentos com capacidades antioxidantes e anti-inflamatórias. O cultivo de microalgas dá-se em sistemas abertos, como em tanques aberto ao ar livre, ou em sistemas fechados, denominados "fotobiorreatores". O cultivo em fotobiorreatores tem certas vantagens como o controlo total dos parâmetros necessários ao cultivo das microalgas como a manutenção de condições adequadas de nutrientes, como azoto, fósforo, e carbono, temperatura, pH, arejamento, agitação do meio, um ambiente biótico estável e condições de luz favoráveis. A luz desempenha um papel essencial, pois é a principal fonte de energia para a fotossíntese, sendo muitas vezes o parâmetro limitante na otimização do cultivo de microalgas já que é progressivamente absorvida pelas células, resultando numa redução da sua disponibilidade nas camadas mais profundas do meio, e favorecendo a respiração celular em detrimento da fotossíntese, por sua vez reduzindo o crescimento das mesmas. Embora a luz solar seja o recurso mais eficiente em termos energéticos para a produção de microalgas, a luz artificial, através de díodos emissores de luz (LEDs), permite um maior controlo das suas condições, como o controlo da intensidade luminosa (quantidade), e dos respetivos comprimentos de onda (qualidade).

Neste estudo, foram cultivadas duas espécies de microalgas, *Nannochloropsis oceanica* e *Phaeodactylum tricornutum*, como também uma espécie de macroalgas, *Porphyra dioica*, na sua fase microscópica (conchocelis) do seu ciclo de vida. Estas algas foram investigadas no que diz respeito à sua eficiência fotossintética em relação à intensidade de luz através de uma curva de fotossíntese-irradiância com o objetivo de determinar as condições de intensidade luminosa para experiências posteriores, na qual *P. dioica* não teve resultados conclusivos e sendo, portanto, excluída. Com os resultados obtidos, foram escolhidos três níveis de intensidade luminosa, 200, 500 e 1000 $\mu mol\ m^{-2}\ s^{-1}$, na experiência seguinte. Esta consistiu em testar vinte e duas combinações de três comprimentos de onda com diferentes níveis de absorção pelas microalgas, 450 (azul), 530 (verde) e 620 (vermelho) nm, e investigar o seu efeito em três concentrações de cultivo (0.2, 2.0 e 5.0 $g\ L^{-1}$) no oxigénio fotossintético dissolvido produzido pelas microalgas. Dos resultados adquiridos desta experiência, foram

criados modelos preditivos estatisticamente significativos, para as duas espécies de microalgas, para cada concentração e intensidade de luz, prevendo a combinação das três qualidades de luz com a melhor eficiência fotossintética.

Através dos modelos criados, foram criados regimes de luz consistindo no uso de condições de luz ótimas face a cada fase de crescimento - fase de adaptação (0.2 g L^{-1}), fase exponencial (2.0 g L^{-1}) e fase exponencial tardia (5.0 g L^{-1}). Em ambos os regimes de luzes foram utilizados 500 µmol m^{-2} s^{-1}. Para *P. tricornutum*, o regime de luz consistiu em usar luz branca quente (controlo) entre 0.2 a 2.0 g L^{-1} e 100% luz vermelha a partir de 2.0 g L^{-1-}, ao passo que para a *N. oceanica*, o regime de luz consistiu em 100% luz vermelha entre 0.2 a 5.0 g L^{-1} e 70% luz vermelha com 30% luz verde após 5.0 g L^{-1}.

Para a validação dos regimes de luz, foi conceptualizado um sistema de luzes, AlgaeLum, adaptado a cultivo de microalgas em frascos Schott de 1L que permite a realização de testes com diferentes qualidades e quantidades de luzes. Quatro replicas deste sistema foram impressas numa impressora 3D de fabricação por filamento fundido (FFF) e posteriormente montadas com os respetivos componentes que as completam.

Na experiência de validação foram usados duplicados para os regimes de luz e duplicados com luz branca quente como controlo para ambas as algas. Esta experiência teve a duração de 14 dias e ambas microalgas passaram por todas as fases de crescimento. No final, foram feitas análises estatísticas para aferir diferenças entre os regimes de luz e controlo relativamente a crescimento (g L^{-1} d^{-1}) e biomassa total (g L^{-1}), e foram realizadas análises bioquímicas para determinar diferenças de concentrações de pigmentos. Com apenas 4 replicados não houve diferenças estatísticas em ambas as microalgas em nenhuma das análises acima referidas.

Por fim, podemos concluir que comprimentos de onda menos absorvidos pelas microalgas (620 nm) resultaram numa maior eficiência fotossintética, principalmente em concentrações elevadas de cultura e curta distância de luz, apesar de esta não ter sido traduzida em um aumento significativo de biomassa total e crescimento destas duas microalgas. Testes com mais replicados são fundamentais para experiências futuras para averiguar se de facto comprimentos menos absorvidos oferecem vantagens no cultivo de microalgas, principalmente em altas concentrações ou em sistemas de cultivo com elevado percurso de luz. A utilização de específicos comprimentos de onda no cultivo de microalgas é um próximo passo na redução do consumo de energia tornando este setor mais sustentável.

List of Figures

List of Tables

List of abbreviations

DO2 %Sat	Dissolved oxygen-saturated
DW	Dry weight
FW	Fresh weight
LED	Light-emitting diode
OD	Optical density
PBR	Photobioreactor
PI	Photosynthetic irradiance
POE	Photosynthetic oxygen evolution
PSII	Photosystem II
RGB	Red green blue
RGBW	Red green blue white
W_f	Final weight
W_i	Initial weight

Table of Contents

1. Introduction

1.1. Market relevance

Photoautotrophic microalgae possess an efficient biological system able to use sunlight as the source of energy to produce high-value organic compounds. Microalgal growth rates are almost 5 to 10-fold faster than conventional food crops and have a higher proportional amount of valuable components such as proteins, lipids, polysaccharides, antioxidants, and pigments (Khoo et al. 2020). This makes them an excellent source for high-value bioactive products for nutraceutical and pharmaceutical applications and as a supplement in human and animal diet. Furthermore, they have a high carbon dioxide and nutrient fixation rate which can be used in flue gas and wastewater remediation treatments (Kumar et al. 2010). The produced biomass can thus become a sustainable feedstock for biofuels (biodiesel, bioethanol, biogas, and biohydrogen) or biomaterials (e.g., biodegradable bioplastics) (Spolaore et al. 2006; Chinnasamy et al. 2012; Nwoba et al. 2019).

The global microalgae market has significantly increased in recent years, from an estimated $0.35 billion in 2010 to $1.11 billion in 2023 (Future Market Insights, 2023; Data Bridge Market Research, 2023) representing a Compound Annual Growth Rate (CAGR) of approximately 9.28%. This growth may be the result of the rising demand and recognition of microalgae potential for sustainable products in various industries.

Despite the growth in the algae market, there are challenges associated with regulatory approval and consumer acceptance. Standardization of production processes, ensuring product safety, and achieving cost-competitiveness remain critical barriers that need to be addressed for broader market adoption (Sharma et al., 2020). Finally, high production costs, primarily due to cultivation, harvesting, and drying methods, are also significant barriers to the competitiveness of microalgal products in the global market. However, technological and biological improvements are expected to lower these costs over time (Wijffels and Barbosa, 2010).

1.2. Factors influencing the growth of phototrophic organisms

Besides light, the source of energy, phototrophic algae requires the maintenance of parameters such as temperature, salinity, nutrient availability, pH, CO_2, and O_2 levels (Darvehei et al. 2018; Quinn et al. 2011). The ease of maintaining and manipulating these parameters makes

microalgae an attractive source of high-value compounds for industrial and environmental applications compared to crops (Rizwan et al. 2018).

Salinity

Salinity stress may have significant effects on the growth and biochemical composition of microalgae (Haris et al. 2022). The machinery to tackle with salinity is engraved in the marine algae genome because of centuries of evolutionary selection. Response and adaptation of cells to different abiotic stresses (e.g., salinity, dehydration, severe osmotic pressure) occur through adaptative mechanisms, such as the changes in the morphological and development patterns as well as physiological and biochemical processes (Shetty et al., 2019). These effects are species-specific, but studies have found that high salt concentration may slow down cell division, reduce cell size, ceases motility, reducing growth rate (Neelam and Subramanyam, 2013).

Temperature

Temperature influences all metabolic processes, and the optimum temperature for a particular algae strain has a pronounced effect on the culture productivity. Heat stress lowers biomass productivity but also lower biomass loss overnight for *Nannochloropsis oceanica* (Carneiro et al., 2020). Temperature also has the effect of changing fatty acid composition. It has been reported that total unsaturated fatty acids decreased with high temperatures (Xin et al., 2011; Thompson, 1996; Carneiro et al., 2020). Those, in microalgae, are necessary for the maintenance of membrane fluidity, and the degree of membrane fluidity depends on the length of fatty acid chains.

pH

During microalgae cultivation under continuous lighting, CO_2 in the medium is actively consumed through photosynthesis. This process decreases the concentration of dissolved CO_2, which shifts the equilibrium of bicarbonate (HCO_3^-) to release more CO_2 for fixation into organic carbon, causing the pH of the medium to rise. Methods for controlling pH include CO_2 injection, buffer addition, and acid/base adjustment. The first two are commonly used in algae cultivation, although the second is not sustainable in large cultivation setups. Using CO_2 is a significant economic consideration to maintain pH levels and, simultaneously increase the carbon availability for photosynthesis. Studies have shown that rising CO_2 concentrations added in the air supply can significantly increase lipid accumulation as well as growth rate in species like *Phaeodactylum tricornutum* and *Nannochloropsis oceanica* (Wu et al., 2015; Ma

et al., 2016). Using CO_2 as a byproduct of an industrial process in the form of, for instance, flue gas can also be implemented as a source of CO_2 to reduce costs, although it requires considering the potential negative effects associated with toxic substances present in this gas on algal growth (Zhu et al., 2014).

Aeration

Aeration is fundamental to maintaining an efficient mix of culture to prevent biofilm formation on the surfaces of the photobioreactor. The prevention of biofilm greatly depends on the position of the air output, airflow, and design of the photobioreactor. From a light distribution efficiency point of view, flat panel photobioreactors are thought to be the most popular due to their highly illuminated surface-area-to-volume ratio, and easy temperature control (Udayan et al., 2022). On the other hand, bubble column airlift photobioreactors are known by their homogeneous culture environment due to their mixing capabilities, efficient CO_2/O_2 mass transfer, and heat transfer (Uyar et al. 2024).

Biochemical composition of the phototroph

Chlorophylls are the most common pigments in microalgae and capture light mainly in the blue and red. Chlorophyll *a* is a pigment found in most of photosynthetic algae and is essential for photosynthesis (Kirk, 1994). Other types of chlorophyll, such as *b*, and *c* expand the range of light absorption, enabling efficient photosynthesis at different depths. Carotenoids are another group of pigments found in microalgae. They perform two primary functions: they broaden the light absorption spectrum, capturing light in the blue-green to green range and most importantly they protect the photosynthetic apparatus from oxidative damage by quenching singlet oxygen and dissipating excess energy as heat (Young and Britton, 1993). Phycobiliproteins, including phycocyanin, allophycocyanin, and phycoerythrin, are found mainly in cyanobacteria and red algae and these pigments are particularly effective in absorbing light in the green, yellow, and orange ranges of the spectrum, making them crucial in deeper water or shaded conditions where light with these wavelengths are predominant (Glazer, 1989). Therefore, light is another factor influencing the growth of microalgae, a topic that will be expanded in the next section.

1.3. Light for phototrophic organisms

Light is the primary energy source driving photosynthesis in microalgae and plants, where photons are absorbed by pigments such as chlorophyll to convert carbon dioxide and water into oxygen and energy-rich organic compounds. However, light is often evaluated based on how it affects human vision rather than its photon energy, which is what determines its effectiveness in photosynthesis. The human eye perceives light in terms of lumens, a measure based on brightness visible to the eye, but photosynthesis is dependent on the number of photons available in the photosynthetically active radiation (PAR) spectrum (400-700 nm). This discrepancy means that conventional light measurements, designed for human use, do not accurately reflect the light's utility for photosynthetic organisms, although this idea has been tackled back in the 1970s (Liu and Van Lersel, 2021). To address this reoccurring problem, Walter and Schöbel (2023) attempted to convert between different light units, such as from lux (lumens per square meter) to photon-based measurements like photosynthetic photon flux density (PPFD, measured in μmol m^{-2} s^{-1}), which is a better indicator of photosynthetic potential. The conversion is not always straightforward because different light sources emit various wavelengths and intensities. Walter and Schöbel emphasize that the use of photon-based light units, rather than relying on imprecise conversion equations, is essential for ensuring standardized measurements, replicability, and comparability between studies on light effects in microalgae.

1.3.1.Light quantity

The Beer-Lambert law is a classical model for light attenuation in cultures, assuming light decreases exponentially as it penetrates through the culture. However, this model does not account for scattering, which is significant in dense microalgal cultures. Light scattering, in combination with absorption, reduces the effective light available for photosynthesis in deeper layers, leading to respiratory activity dominating over photosynthetic processes. Studies by Cornet et al. (1994) improve upon this model by including bi-directional light transfer, which better reflects light behavior in dense algal cultures. Research by Berberoglu et al. (2008) and Pottier et al. (2005) also explores how light scattering and absorption impact microalgal culture productivity, further underscoring the importance of models that account for both factors.

Pigments, primarily chlorophylls, carotenoids, and phycobilins, are the main molecules absorbing visible light in microalgal cells. Their absorption spectra determine how efficiently microalgae can utilize specific wavelengths of light. The type and concentration of pigments within the microalgal cells influence how light is absorbed, making it crucial to develop models

that account for varying pigment compositions across species. Studies like those by Katsuda et al. (2000) and Berberoglu et al. (2008) emphasize the need for a more detailed understanding of pigment absorption dynamics in relation to the incident light spectrum.

As light penetration decreases with culture depth, increasing light intensity to overcome self-shading can lead to a new challenge—photoinhibition, a condition where excessive light damages the photosynthetic machinery, particularly photosystem II (PSII).

Photoinhibition refers to the light-induced damage to PSII in microalgae, when they are exposed to light intensities that exceed their photosynthetic capacity. According to Tyystjärvi (2013), photoinhibition occurs when the rate of PSII damage, induced primarily by light, surpasses the rate of its repair, leading to a decrease in photosynthetic efficiency. This process is particularly problematic under strong light conditions, where excessive energy generates reactive oxygen species (ROS), which then cause oxidative damage to the D1 protein in PSII. To maintain functional photosynthesis, the damaged D1 protein must be continuously degraded and replaced, but if the repair mechanisms cannot keep up, photoinhibition occurs, leading to a reduction in photosynthetic performance.

Photoinhibition acts as a protective mechanism, limiting the damage caused by high-light conditions. Under low to moderate light, the repair rate is generally sufficient to counterbalance the damage. However, under excessive light or environmental stress, repair cannot match the rate of PSII damage. Murata et al. (2012) further support this concept, explaining how light-induced PSII damage is mitigated through repair mechanisms, but if the light-induced damage rate surpasses the repair capacity, photoinhibition leads to a decline in overall photosynthetic capacity. This is particularly significant when microalgae are exposed to high light intensities to overcome self-shading, as the increased intensity can induce photoinhibition if not properly managed.

Photoprotection mechanisms, such as the xanthophyll cycle, play a critical role in mitigating the effects of excessive light on photosystem II (PSII), reducing photoinhibition risk. The cycle involves converting specific pigments to dissipate excess energy as heat, preventing the formation of ROS that cause oxidative damage to PSII. According to Short et al. (2023), this photoprotective "memory" allows microalgae to dynamically respond to fluctuating light, enhancing resilience and maintaining photosynthetic efficiency.

Thus, photoinhibition represents a balance between damage and repair in the photosynthetic machinery and exceeding the repair capacity leads to decreased efficiency in PSII and overall photosynthesis, particularly under high-light environments. This balance is critical for optimizing growth in photobioreactor systems and other cultivation setups.

1.3.2.Light quality

N. oceanica and P. tricornutum absorb light from the photosynthetically active radiation (PAR) spectrum (400 to 700 nm) (Nunez and Quigg, 2016). *N. oceanica* primarily contains chlorophyll *a*, along with accessory pigments like violaxanthin, *β*-carotene, and zeaxanthin, which are crucial for light absorption and photoprotection (Van Wagenen et al., 2012). On the other hand, *P. tricornutum* has chlorophyll *a* and *c*, as well as fucoxanthin, which is characteristic of diatoms and brown algae (Lepetit et al., 2010).

Changes in the light conditions can influence the growth rates of microalgae and the accumulation of different high-value components such as carotenoids, lipids, carbohydrates, and proteins (Maltsev et al. 2021; Nzayisenga et al. 2020). The light wavelengths and light intensity are responsible for changes in microalgae pigmentation, morphology, and biochemical composition. This adaptability allows microalgae to optimize their energy uses under different environmental conditions. Changes in light quality can influence the ratio and total content of chlorophylls *a* and *b* within algal cells; for instance, when exposed to blue (430 to 450 nm) and red light (630 to 660 nm), microalgae increase their chlorophylls content, optimizing their capacity to capture these wavelengths (Schulze et al. 2016). Regarding carotenoids, exposure to high light intensities and blue light often results in increased biosynthesis of these compounds, which help dissipate excess energy and protect chlorophyll molecules from degradation (Young and Britton, 1993). These pigments are not only essential for photosynthesis but also valuable as natural colorants and antioxidants in the food and cosmetics industries (Christaki et al., 2013). Wavelengths in the blue and red have been shown to enhance lipid production in various species including *Nannochloropsis spp.* (Simionato et al. 2011; Ma et al. 2016). Blue and white light can also influence the saturation level of fatty acids, which is crucial for both nutritional and industrial applications (Xu et al. 2017). Light quality also influences the biosynthesis of proteins and carbohydrates. For instance, red light has been associated with increased carbohydrate accumulation in some species (*Arthrospira platensis* often referred to as “Spirulina”), which can be beneficial for bioethanol production and other bioenergy uses (Chen et al. 2011). Conversely, both red and blue can stimulate protein production, also depending on the species, which has implications for using algae in animal feed and human dietary supplements (Converti et al. 2009; Rodolfi et al. 2009). Red light (660 nm) is also associated with increased biomass productivity, lipid accumulation and thylakoid expansion, leading to a more efficient light absorption; in addition, it also been suggested that it can impact cell morphology (Sharma et al., 2020).

The synthesis of secondary metabolites, including antioxidants, vitamins, and other valuable components (pharmaceutical and nutraceutical applications) is also affected by electromagnetic radiation wavelengths. For example, UV radiation can increase the biosynthesis of mycosporine-like amino acids, known for their UV-protective and antioxidant properties (Carreto and Carignan, 2011).

Variations in light intensity and attenuation across experimental setups may lead to inconsistent results regarding microalgal growth and pigments accumulation studies, even when using the same light wavelengths. Different culture concentrations have distinct light and dark zones within cultures, causing uneven exposure that affects photosynthesis, pigment production, and growth. Hong et al. (2023) note that such differences can alter experimental outcomes. Consequently, studies with higher light intensities or different reactor designs may report enhanced growth or distinct physiological responses, which are not directly comparable to results from lower intensity setups. When investigating the effects of different light wavelengths on microalgae, it is essential to consider the culture concentration and light path, as these factors influence the distribution of light and dark zones in the culture. The light path refers to the distance light has to travel through the algal culture, which is crucial for optimizing the growth of microalgae. Therefore, both culture concentration and light path must be accounted for when comparing results across studies to ensure valid and consistent findings.

1.4. LED-lit Photobioreactors

Photobioreactors are specialized closed systems designed for the growth and maintenance of photosynthetic organisms promoting efficient conversion of energy biomass light via photosynthesis. They allow the growth of these organisms under conditions such as pH, salinity, temperature, light quality and quantity, air and CO2 intake, nutrient intake, turbidity that can be monitored with a high degree of precision. They also limit evaporation, resulting in lower water losses, higher productivity and biomass concentrations when compared to open systems (Udayan et al., 2022; Sirohi et al 2022). To artificially illuminate PBRs, fluorescent lamps or LEDs are typically employed either internally or externally (Glemser et al. 2015; Heining and Buchholz, 2015). Photobioreactors are typically constructed using transparent materials like glass, plexiglass, and polycarbonate to allow light penetration, coming in various configurations, such as bubble columns, helical tubes, stirred tanks, airlifts, flat panels, and tubular reactors (Chang et al., 2017).

The strategic use of artificial light, using light-emitting diodes (LEDs), has become increasingly significant in microalgae cultivation since LEDs offer the ability to provide specific light wavelengths and intensity. LEDs can be tailored to improve growth and enhance the biochemical composition of microalgae, such as pigments, lipids, proteins, carbohydrates, and other valuable secondary metabolites. LEDs are highly energy-efficient compared to other artificial light sources, decreasing energy costs up to 80% compared to incandescent bulbs and having up to 50 times longer lifetimes (Cho et al., 2017). They also allow to be placed in tighter places closer to the algae culture without the risk of overheating. Moreover, LEDs can be tailored to emit in a narrow spectrum of light, which can be set to match with specific absorption peaks on the targeted microalgae (Cuaresma et al., 2011).

At an industrial scale, such as in open ponds and tubular photobioreactors, sunlight is often used to illuminate the photobioreactors to reduce energy costs. However, in lab-scale photobioreactors, artificial light can be used for illumination because experiments are often carried out indoors. Artificial light allows higher concentrations of algal biomass and of the target products due to its capacity to emit light at specific wavelengths that trigger the biosynthesis of specific compounds (Singh and Mishra, 2022).

Having precise control over these light parameters can significantly influence microalgae's productivity and have application in the use of lab-scaled photobioreactors (PBRS) being crucial for researching and developing optimal light conditions for microalgae cultivation. PBRs allow precise control over simulated environmental conditions such as light (photoperiod, light wavelength and intensity), CO_2 intake, air intake, nutrient intake, new media intake, turbidity, pH, temperature. Under these controlled conditions, it is also possible to simultaneously measure the microalgae cultivation parameters (e.g., biomass concentration, optical density), while controlling sedimentation or flocculation of the culture (AI-Dailami et al., 2022).

Lab-scale PBRs allow researchers to isolate the effects of light from another variable, being of great use when testing the effect of different light wavelengths, light intensity, and photoperiods on algae growth and specific component synthesis. By optimizing these conditions at a smaller scale, it is possible to study the feasibility of scaling up successful protocols to larger, commercial systems (Amaral et al., 2021).

The cost of lab-scale PBRs can range from a hundred to several thousand dollars, depending on the complexity of the system and the solutions they provide. Although the investment in these systems is justified by the precision they offer in experimental conditions, which is crucial

for reliable and reproducible results, multiple reactors are required to be operated simultaneously to achieve a high number of replicates and improve the consistency of results.
In the cultivation of algae, as light is often the main energy source, it is one of the primary limiting factors (or bottlenecks) on productivity and scalability (López et al. 2018; Ma et al., 2022).
Recent advances focus on improving light distribution in cultures with the implementation of techniques such as reflective materials, integration of light-diffusing fibres inside the culture, pulsing light sources, and adaptive light systems that adjust light intensities based on real-time culture density measurements, to enhance light penetration and reduce the self-shading effect of one cell with regard to its neighbouring algal cells (Richmond, 2013; Schulze et al. 2020). Despite the implementation of new techniques, novel photobioreactor designs arise to allow for a more uniform light distribution and scalable options (Posten, 2009). However, there are some drawbacks associated with photobioreactors, such as high production and maintenance costs, demanding cleaning requirements, and challenges related to light penetration. Fouling is also an important factor to keep in mind, because of the stickiness of some microalgae to the vessel walls, which can result in the accumulation of organic material and light obstruction to the culture. Regular sterilization, chemical cleaning, or antifouling methods such as using plastic pellets and increased hydrodynamics, are required (Yen et al., 2019; Zhou et al., 2020). PBR designs, such as flat panels, minimize the light path by having thin layers of culture illuminated by one or two sides, which improves light penetration, specially at high algal concentrations. On the other hand, designs, such as tubular and vertical columns, have longer light paths and are heavily dependent on mixing to ensure even light distribution through the culture or, in some cases, the use of internal illumination (impermeable LEDs or fiber optics) (Posten, 2009). The second type of PBR is more prone to creation of dark zones due to the shading effect caused by its vertical layout.

1.4.1.Lab-scale photobioreactors

Lab-scale photobioreactors are commonly used to test the effect of different parameters on algae in a controlled system, to either investigate the effect of isolated parameters on algal growth, photosynthesis efficiency or accumulation of valuable biochemical compounds (Cañedo et al., 2016). For light quality and quantity experiments, a variety of light conditions are usually tested using multiple replicates rather than different trials, as algae cultivation can take up to two weeks to progress from the lag phase to the exponential phase. Using replicates

makes more efficient the use of time, but lab-scale photobioreactors are often expensive, limiting the number of simultaneous replicates. This constraint leads researchers to build custom light setups, which are labour-intensive and may create inconsistencies in light conditions across replicates, potentially affecting experimental reproducibility and the robustness of the results (Figure 1).

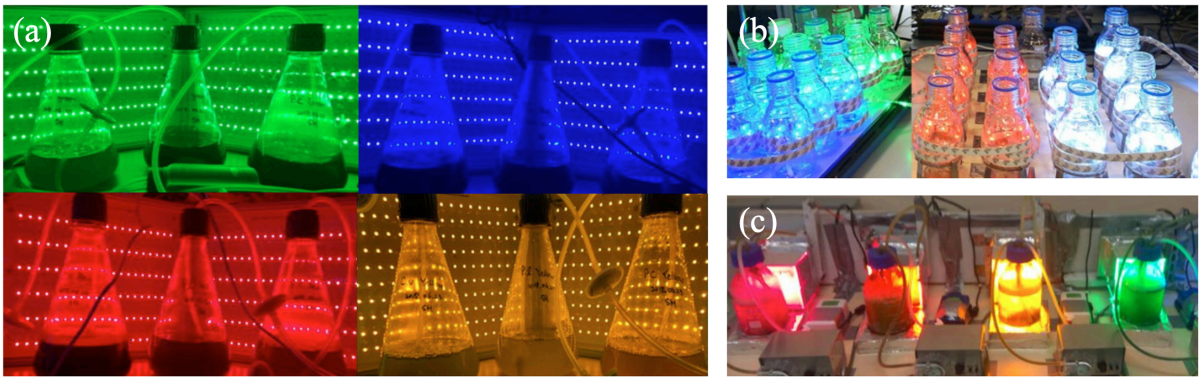

Figure 1 Comparison of various custom-built light setups used in microalgal cultivation experiments to investigate the effects of light quality: (a) Kim et al. (2019); (b) Fernandez-Marchante et al. (2018); and (c) Angelov and Lecheva (2023). These setups highlight the diverse approaches to light experimentation and undercover the challenges of achieving reproducibility and uniform conditions across replicates.

There is a continuous need for development of a solution that accommodate globally used cultivation vessels like Erlenmeyer or Schott flasks, ensuring accessibility and reproducibility across different laboratories worldwide. It should be low-cost to allow replicability and easy to use to minimize labour time at high replicate volumes. The system should provide homogeneous light distribution from multiple angles, be capable of delivering variable light intensities, wavelengths, and photoperiods, while shielding the culture from external light interference. Additionally, it should not disrupt other controlled parameters such as temperature, aeration, pH, and CO_2 delivery, ensuring consistent experimental conditions.

1.5. Justification of the dissertation

Although there has been an increase in number of studies regarding the cultivation of microalgae under different light qualities and quantities using LEDs, there are still knowledge gaps on how microalgae respond to light. Furthermore, a few examples of studies regarding different light qualities and quantities were found for *P. tricornutum* and *N. oceanica* but require further validation because authors did not adapt light conditions to biomass concentration in the culture (Duarte at el., 2021; Dong et al., 2023; Rao et al., 2022). As these

species belong to different evolutionary lines and have different accessory and main pigments, they may differ in optimal light wavelengths and light intensity for increased growth.
Lastly, there is a need for affordable photobioreactors to test light conditions on microalgae.
Hence, this thesis aims to improve light delivery and for artificial light-based microalgae cultivation and develop a low-cost photobioreactor to test rapidly different wavelengths and combinations thereof.

1.6. Objectives

To fill the gaps in the current state of the art, the main objective of current dissertation was to explore the application of different absorbed wavelengths to improve growth in *Phaeodactylum tricornutum*, *Nannochloropsis oceanica*, and *Porphyra dioica*. Hence, a specific objective of the present dissertation was to investigate the effect of different combinations of light wavelengths and light intensities on photosynthetic oxygen activity. The second objective was the selection of light wavelength combinations that performed better to create a predictive light model for microalgae growth and its application on each cultivation stage to improve growth.
With this purpose in mind, the present study investigates and discusses how the absorbance of high and low-absorbed light wavelengths can be implemented to improve productivity during each algae growth stage and at different light-path cultivation systems. The obtained conclusions may result in optimized methods for efficient large-scale production. Lastly, the third objective was the development of a light system that could turn Schott flasks, which are often used for microalgae cultivation, into an affordable and efficient photobioreactor for light conditions experiments. The invented prototype may offer a reliable way to conduct light experiments, due to its affordability, mainly due to the low-cost components, its practicability, replicability, and reliability.

2. Material and methods

2.1. Algae

For this experiment, three marine algal species were cultivated and tested at the GreenCoLab – Associação Oceano Verde laboratories, University of Algarve, Portugal, namely *Nannochloropsis sp.* (Eustigmatophyceae), *Phaeodactylum tricornutum* (Bacillariophyceae) provided by Allmicroalgae S.A., Leiria, Portugal, and conchocelis phase of *Porphyra dioica* (Rhodophyta) by Algaplus, Ílhavo, Portugal. The culture medium used for the algae was composed of artificial seawater (salinity 33 ppt) and 4 different solutions: micronutrients (1.0 µmol L^{-1} $ZnCl_2$; 1.0 µmol L^{-1} $ZnSO_4{-}H_2O$; 1.0 µmol L^{-1} $MnCl_2{\bullet}4H_2O$; 0.1 µmol L^{-1} $Na_2MoO_4{\bullet}2H_2O$; 0.1 µmol L^{-1} $CaCl_2{\bullet}6H_2O$; 0.1 µmol L^{-1} $CuSO_4{\bullet}5H_2O$; 6.4 µmol L^{-1} EDTA-Na; 2.0 µmol L^{-1} $MgSO_4{\bullet}7H_2O$), iron (20.0 µmol L^{-1} EDTA-Na; 20.0 µmol L^{-1} $FeCl_3$) and macronutrients (2000 µmol L^{-1} $NaNO_3$; 100.0 µmol L^{-1} KH_2PO_4). Silica (2023 µmol L^{-1} Si) was additionally supplied to *P. tricornutum* cultures. *Porphyra dioica* was sent by Algaplus together with its respective in-house growth medium.

A semi-continuous cultivation system and an experimental setup were established in GreenCoLab's facilities to maintain these algae at specific concentrations and conduct the following experiments.

2.2. Cultivation system

All the algae were scaled up in three 1-L bubble column PBR with water jackets (designed by GreenCoLab), each with 900 mL (Figure 2). These PBRs were maintained in semi-continuous cultivation at a targeted biomass set point (e.g., 0.2, 2.0, and 5.0 g L^{-1}) before starting the photosynthetic oxygen evolution (POE) experiment.

To maintain the temperatures of 22ºC to *P. tricornutum* and *N.oceanica,* and 17ºC to *P. dioica*, a chiller (JULABO GmbH, Seelbach, Germany) was connected in parallel to the water jackets of all three PBRs. Continuous illumination was provided to all PBRs LED strips (warm white light) from one side to optimize growth. The same light intensity was used in the POE experiment. All the light intensity values were captured using a LI-1500 Light Sensor Logger (LI-COR Biosciences, Lincoln, NE, USA) equipped with a spheric quantum sensor LI-190R (LI-COR Biosciences, Lincoln, NE, USA) immersed in the vessels filled with water.

To compensate for water evaporation, an air humidifier system was incorporated into the air supply line using a linear air pump (Charles Austen, ET 120). Each PBR was equipped with a

flowmeter to ensure uniform airflow of 800 ml min^{-1}. Glass fiber filters Whatman with a pore size of 0.7 µm were used in the air supply lines to prevent contamination. Additionally, a pH system was integrated. Every PBR featured a H12114P pH probe (Hanna Instruments, Woonsocket, RI, USA) connected to a BL931700 pH controller (Hanna Instruments, Woonsocket, RI, USA), which displayed the real-time pH. This controller was connected to a solenoid valve MF5 (Pneumax Spa, Lurano, Italy) in the CO_2 supply line. When the pH exceeded the set point of 8.0, these valves would open, injecting CO_2 into the culture and reducing the pH until it underwent the setpoint (Figure 3).

P. tricornutum and *N. oceanica* were cultivated in the cultivation system under a light intensity of 200 µmol m^{-2} s^{-1}, to achieve concentrations of 0.2 and 2.0 g L^{-1} and adjusted to 500 µmol m^{-2} s^{-1} to achieve 5.0 g L^{-1}. *P. dioica* was maintained at a light intensity of 100 µmol m^{-2} s^{-1}.

Once the targeted biomass was achieved, the cultivation system was connected to the photosynthetic chamber in which the POE experiment took place.

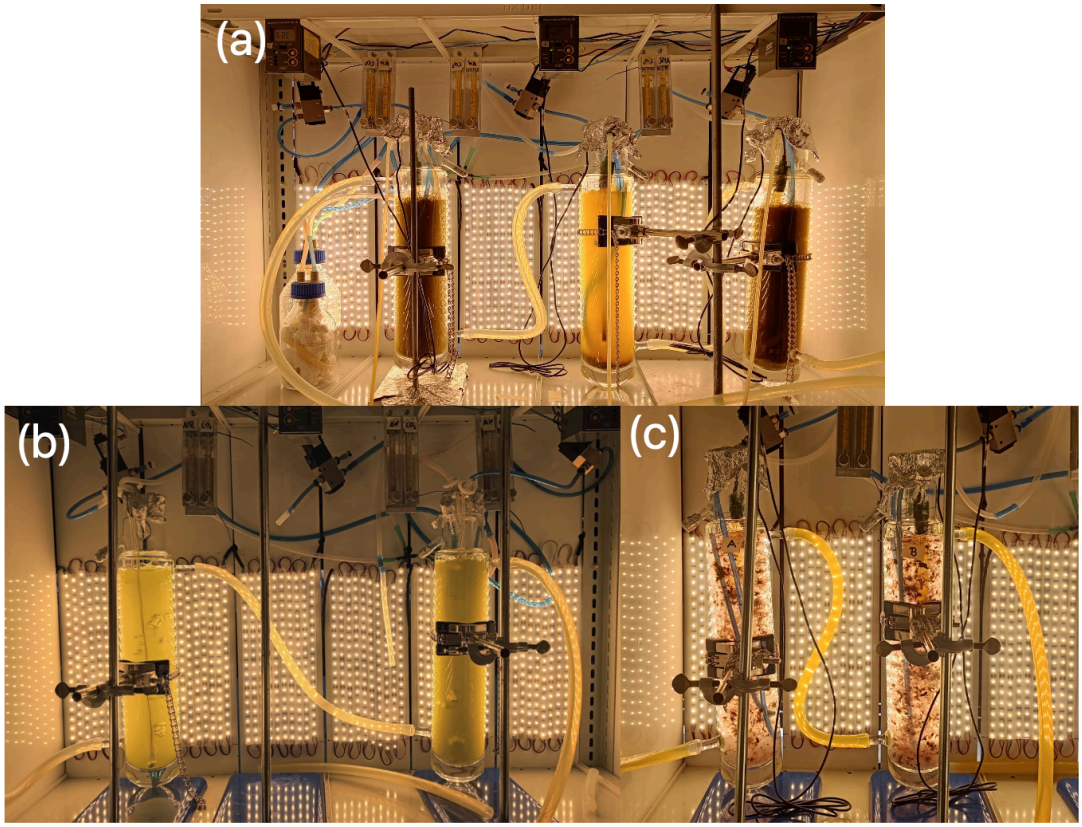

Figure 2 Cultivation system with 3 growth stages of *Phaeodactylum tricornutum* at 5.0, 0.2, and 2.0 gDW L^{-1} , respectively. (b) Cultivation system with 2 growth stages of *Nannochloropsis oceanica* at 0.2 and 2.0 gDW L^{-1}. (c) Cultivation system with 2 replicates of *Porphyra dioica* at 20 gFW L^{-1}.

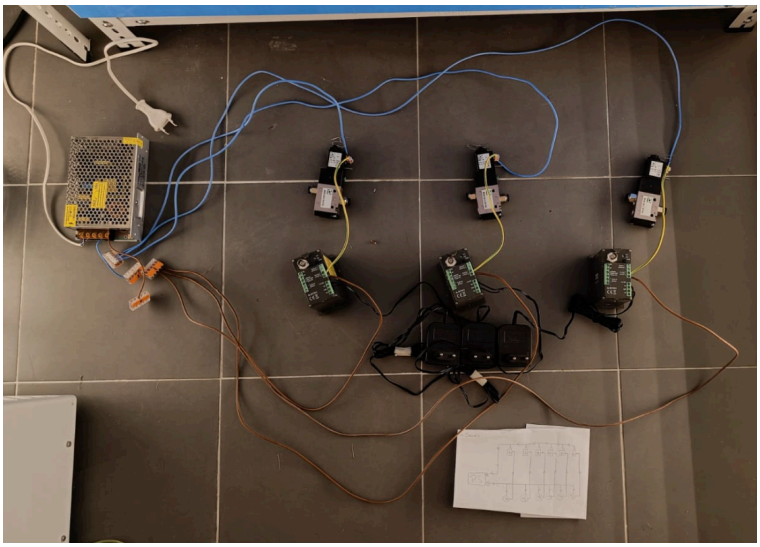

Figure 3 Electronic apparatus arranged in parallel incorporating 3 solenoids powered by a power supply (230VAC-24VDC) and connected to 3 pH controllers powered by individual power supplies (230VAC-12VDC) to automate pH levelling of the algae cultures.

2.3. Photosynthetic chamber

2.3.1. Photosynthetic measurements

POE tests were conducted within a specially designed glass photosynthetic chamber (Figure 4). This vessel comprises three individual chambers, each with a volume of 200 mL and a light path of 20 mm. The central chamber's purpose is to contain algae culture, while the adjacent chambers are connected to the cooling system of the cultivation setup, maintaining the same temperature as the stock cultures to avoid thermal shocks of the algae tested.

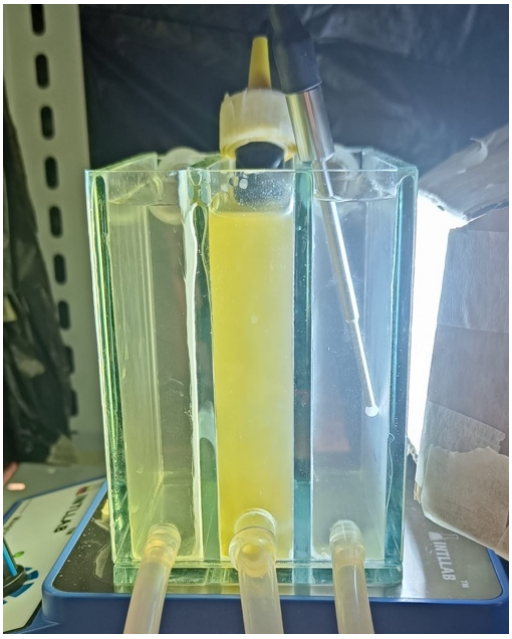

Figure 4 Photosynthetic chamber filled with *Phaeodactylum tricornutum* (0.2 g L^{-1}) in the middle chamber and filled with distilled water in the adjacent chambers at 22ºC under 500 µmol m^{-2} s^{-1}).

Below the photosynthetic chamber, a magnetic stirrer was placed to ensure continuous mixing of the algae medium. Within the chamber, a Surveyor™ analog dissolved oxygen probe (Atlas Scientific, New York, USA) was installed, interfacing with an oxygen meter. This component translated electrical signals to analog outputs, which were then processed in Termite (Version 3.4, CompuPhase, Netherlands), a computer software used to read and store data from RS232 terminals. This setup allowed dissolved oxygen readings at one-second intervals. Additionally, the quantum sensor was also installed within the chamber to measure the light intensity inside the culture during the POE experiments.

On the exterior, a multispectral LED (Heliospectra DYNA, Gothenburg, Sweden), used to deliver the exact ratio of different light wavelengths to the culture, was aligned with a hand-made light funnel (Figure 5) directed at the photosynthetic chamber. To eliminate any light pollution from the ambient lights, the entire experimental setup was covered by black plastic foil. Lastly, for a practical culture filling and draining, a silicon tubing was connected to the photosynthetic chamber. The entire setup is schematized in Figure 6.

Figure 5. Experimental system with an empty photosynthetic chamber under a wavelength combination ratio of 50% blue (450 nm) and 50% red (620 nm) at 200 µmol m^{-2} s^{-1}.

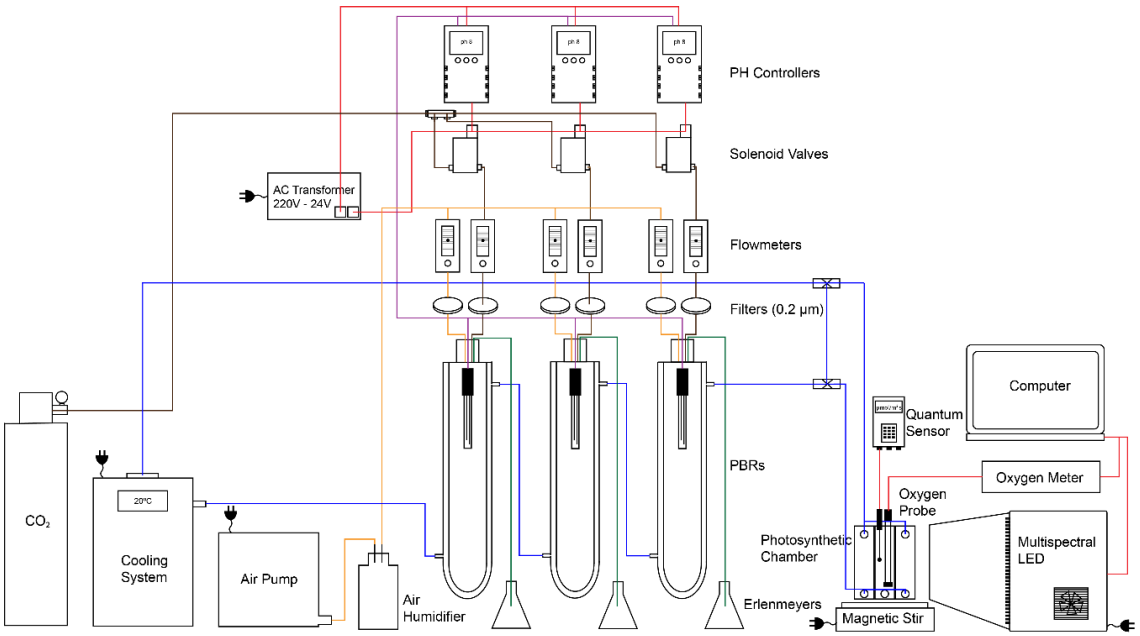

Figure 6 Simplified schematic of the cultivation and experimental systems setup. Blue lines represent the water circulation, brown lines the CO2 circulation, orange lines the air circulation, green lines the algae culture circulation, and purple and red lines represent the electric wires connections.

2.2.2.Oxygen evolution trials

A photosynthesis–irradiance (PI) curve, which shows the correlation between light intensity and photosynthetic rate was established for each algae species to determine the most appropriate light intensities for the POE experiments. Photosynthesis-Irradiance (PI) curves were generated for the three algae species. The PI curve typically exhibits three distinct phases: the photo-limited phase at low light intensities, the light-saturated phase where photosynthetic rate peaks, and the photo-inhibitory phase at high light intensities (Darvehei et al., 2018).

All three algae were subjected to the same procedure. *P. tricornutum* and *N. oceanica* stocks were acclimatized to 200 µmol m^{-2} s^{-1} and *P. dioica* to 100 µmol m^{-2} s^{-1}. For each alga species, two PBRs were used, each with a different biomass concentration. A volume of 200 mL of culture was poured into the photosynthetic chamber for 15-20 minutes under various levels of light intensities from 50 up to 1000 µmol m^{-2} s^{-1} to measure POE. Each POE at its respective light intensity was then plotted to create a photosynthesis–irradiance curve.

Once defined the light intensities to be tested from the PI curves, twenty-two light combinations with different ratios of three light wavelengths (620 nm – red, 530 nm – green, and 450 nm – blue) were selected to be accessed in the POE experiment (Table 1, see Annex 1). Each of these conditions was tested at three light intensity regimes: 100, 500, and 1000 µmol m^{-2} s^{-1}).

Table 1 Setup with 22 light wavelength combinations to be tested and the respective ratio of red (620 nm), green (530 nm), and blue (450 nm) light.

Light wavelength combination	Red ratio (620nm)	Green ratio (530nm)	Blue ratio (450nm)
1	1	0	0
2	0	0	1
3	0	1	0
4	0.5	0.5	0
5	0.5	0	0.5
6	0	0.5	0.5
7	0.8	0.1	0.1
8	0.1	0.1	0.8
9	0.1	0.8	0.1
10	0	0.7	0.3
11	0	0.3	0.7
12	0.7	0.3	0
13	0.7	0	0.3
14	0.3	0.7	0
15	0.3	0	0.7
16	0.1	0.6	0.3
17	0.1	0.3	0.6
18	0.6	0.1	0.3
19	0.6	0.3	0.1
20	0.3	0.1	0.6
21	0.3	0.6	0.1
22	0.33(3)	0.33(3)	0.33(3)

Three algae biomass concentrations were selected: 0.2, 2.0 and 5.0 g L^{-1}, representing the early, middle and late exponential phases, respectively. All the conditions are schematically depicted in Figure 7.

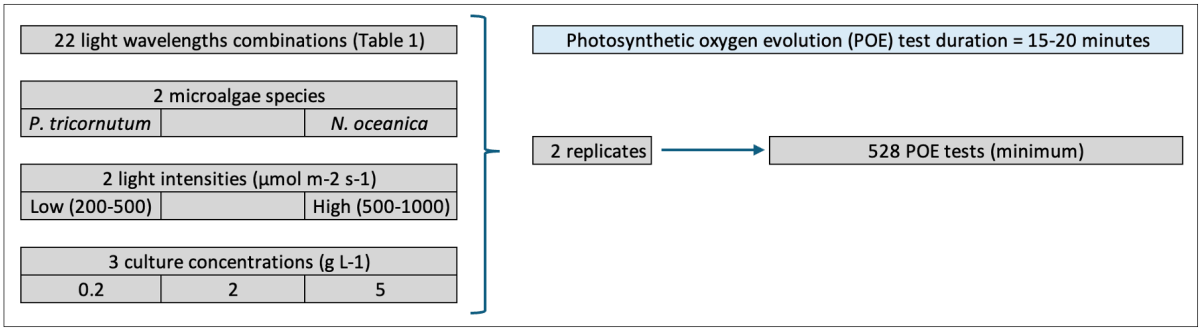

Figure 7 Schematic of all conducted photosynthetic oxygen evolution tests (POE).

For each POE test, aliquots of 250 mL of algae culture were drained from a designated tubular PBR and transferred to a 500 mL Erlenmeyer flask. Approximately 30 mL of algae were poured into the photosynthetic chamber to rinse any remains from prior tests. Subsequently, the

chamber was filled with 200 mL culture. One light condition was selected from the light conditions table and measured the light intensity to ensure the correct light condition was applied. The oxygen evolution was monitored over a period of 10-20 min. Upon completing the test, the chamber was drained, and the culture was returned to one PBR where the culture was maintained to re-acclimatize to the light condition before being reintroduced in the POE tests. For the next test, the algal culture was drained from another PBR to maximize the amount of time that the subjected algae had to photo-acclimatize to the standard cultivation system conditions as detailed in Section 2.2.

Photosynthesis-irradiance (PI) curves were conducted on diluted (0.2 gDW L^{-1}) and concentrated (2.0 gDW L^{-1}) *P. tricornutum* and *N. oceanica* cultures by exposing them to increasing light intensities (50-1000 µmol m^{-2} s^{-1}). On the other hand, *P. dioica* was tested in a diluted (10 gFW L^{-1}) and concentrated (20 gFW L^{-1}) medium. The POE was then measured for each condition.

2.3. Validation trial light regimes

P. tricornutum and *N. oceanica* were cultivated in Schott flasks under defined light conditions. Based on the data collected from the POE experiments, statistic models were developed to predict the optimal combination of red, green, and blue light for the growth of the targeted algae species under each growth stage (lag, exponential, and late exponential phase). These predictive models for each growth phase were integrated to establish a light regime, ensuring optimal light conditions throughout all three growth phases and compared with warm white light at the same light intensity. Similar to the conditions in the POE experiments, systems for air humidification, cooling, and pH control were implemented to maintain a temperature of 22º C, a pH of 8.0, and an airflow of 800 ml L^{-1}.

The light regime for *P. tricornutum* cultivation started with warm white at 500 µmol m^{-2} s^{-1} from day 0 until reached 2.0 g L^{-1} upon which the light regime was changed to 100% red light (620 nm) until the end of the experiment (Figure 8). The light intensity was measured from the inside of the cultivation flask using the spherical quantum sensor connected to the data logger. For *N. oceanica*, the cultivation started with 100% red light at 500 µmol m^{-2} s^{-1} and changed to 75% red and 25% green light (530 nm) until the end of the experiment (Figure 9). All experiments were carried out in duplicates and repeated twice.

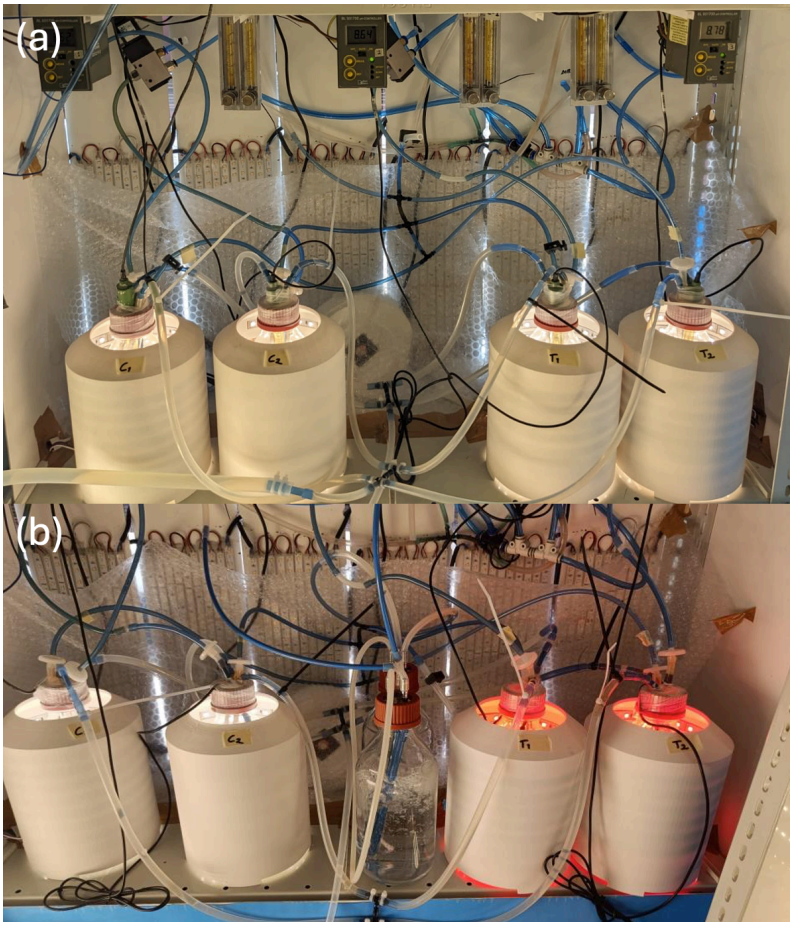

Figure 8 Cultivation setup of the control warm-white and light regime experiment on *Phaeodactylum tricornutum*. Image (a) shows the setup from 0.2 g L^{-1} to 2.0 g L^{-1}, using warm white light, 500 µmol m^{-2} s^{-1}, and image (b) shows the setup past 2.0 g L^{-1}, using 100% red light, 500 µmol m^{-2} s^{-1}.

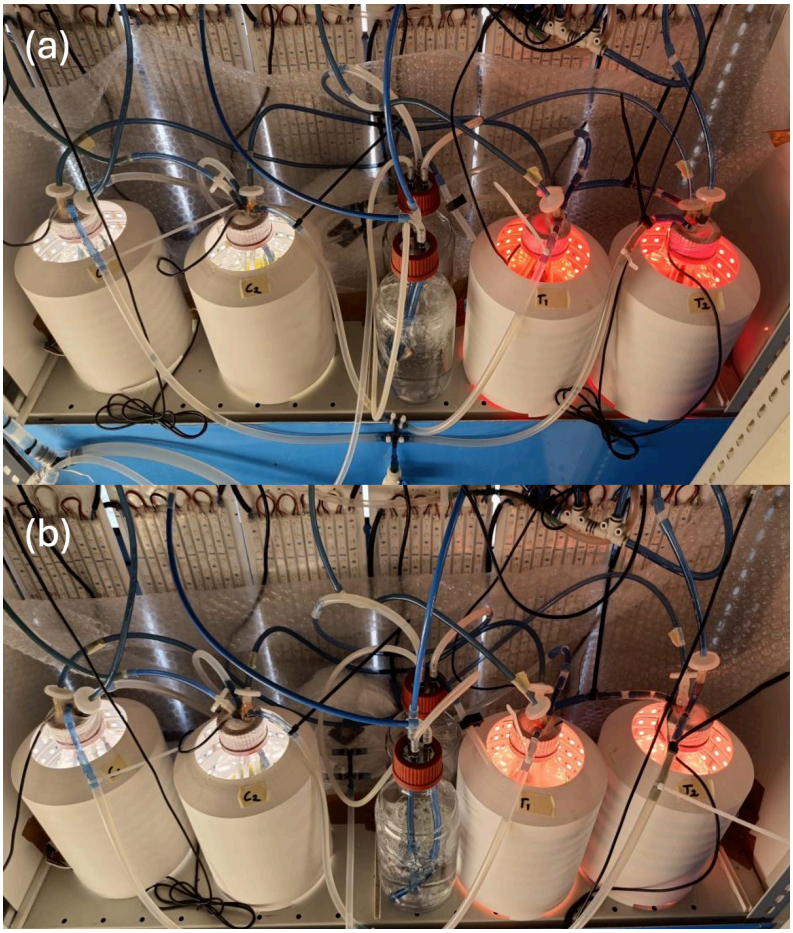

Figure 9 Cultivation setup of the control warm-white and light regime experiment on *Nannochloropsis oceanica*. Image (a) shows the setup from 0.2 g L^{-1} to 5.0 g L^{-1}, using 100% red, 500 µmol m^{-2} s^{-1} light in the light regimes replicates, and image (b) shows the setup past 5.0 g L^{-1}, using 75% red light and 25% green light, 500 µmol m^{-2} s^{-1}.

2.4. Culture parameter

2.4.1.Biomass-OD correlation

The optical density (OD) of *P. tricornutum* and *N. oceanica* cultures was measured at a wavelength of 750 nm using the spectrophotometer. To ensure that the OD measurements were within the linear range of the spectrophotometer's calibration, the cultures were appropriately diluted to achieve OD values between 0.2 and 0.8. Subsequently, the OD of the undiluted sample was determined by dividing the measured value by the dilution factor. This approach enabled the establishment of a reliable correlation between the measured OD and the actual dry weight (DW) biomass concentration of the microalgae cultures.

For monitoring culture growth and correlating it with total dry weights, the method employed was adapted from Zhu and Lee (1997) with minor modifications. Glass fibre filters Whatman with a pore size of 0.7 µm were used to determine total dry weight. The filters were washed

with ammonium bicarbonate (31.5 g to 1000 mL of distilled water), dried in an oven at 60 °C for 48 hours, cooled in a vacuum desiccator (30 min), and then weighed and registered the filter weight (W_i). Culture aliquots of 10 mL were collected, filtered through the prepared filters, washed with ammonium bicarbonate, dried again in an oven at 100 °C for 48 hours, cooled, and then weighed the filter with culture (W_f) to calculate the total dry weight of the sample. The DW was calculated using Equation 1:

$$\text{DW (g/L)} = \frac{Wf - Wi\ (g)}{Sample\ (L)} \quad (1)$$

Because homogenous dilution in a cuvette for OD measurement was not possible for *Porphyra dioica*, fresh weight (FW) was used instead.

2.4.2.Absorption spectrum

Qualitative absorption spectra were determined by spectrophotometry for *P. tricornutum* and *N. oceanica* to compare the absorption of blue (450 nm), green (530 nm), and red (620 nm). The absorption was measured using 10-nm steps from 400 to 750 nm (Figure 10). The absorption spectrum of a cuvette containing growth medium in artificial seawater (33 salinity) was used as blank.

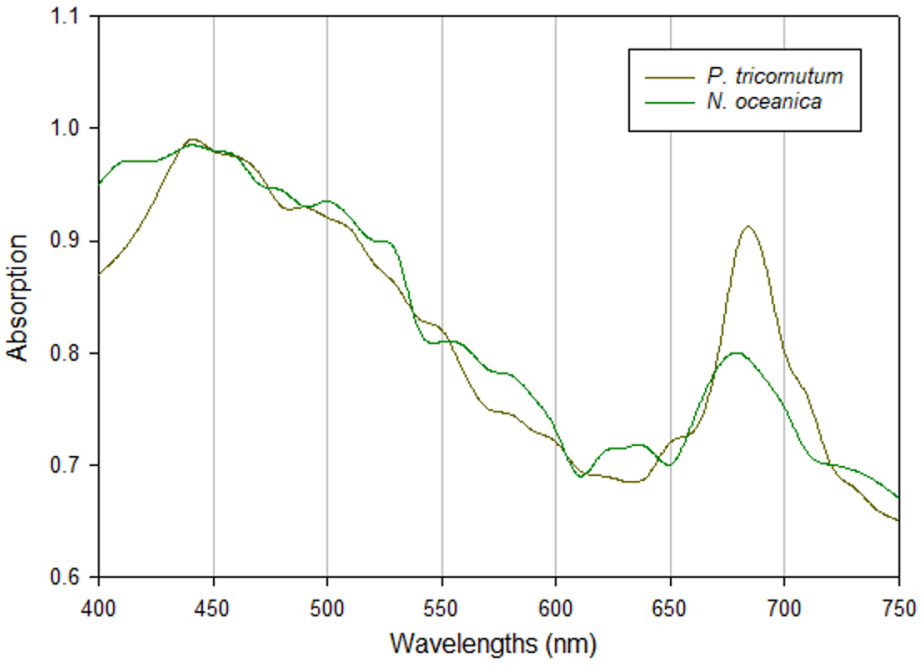

Figure 10 Absorption spectrum of *Phaeodactylum tricornutum* and *Nannochloropsis oceanica* from 400 nm to 750 nm using 10-nm steps.

2.5. Pigment analysis

At the end of the light regime in the cultivation experiment, aliquots of 50 mL were sampled from all treatments into 50 mL Falcon tubes. The tubes were then centrifuged at 15,000 *g* for 5 minutes (Centrifuge 5430 R, Eppendorf, Hamburg, Germany). After centrifugation, the supernatant was removed, and the pellets were immediately frozen at -80 ºC (ULF400 -86 Freezer, BWR, Carnaxide, PT) for further analysis. For the determination of total carotenoids and chlorophyll, all the extraction process was carried out under low light conditions and on ice. The pellets were initially freeze-dried (LyoMicron, Coolvacuum, Barcelona, Spain) for 24 hours, weighed (5 mg each), and placed into 2 mL Eppendorf tubes. Each tube received 0.5 mL of glass beads (425-600 µm diameter) and 1 mL of 100% methanol containing 0.03% butylhydroxytoluene (BHT) as an antioxidant. The samples were then homogenized in a Retsch MM 400 mixer mill at 30 Hz for three cycles of 1 minute each to disrupt the cells. Afterwards, the samples were centrifuged at 15,000 *g* for 5 minutes. The clear supernatant was transferred to a new Eppendorf tube. This extraction process was repeated 4-5 times until the supernatant and the. Pellet was colourless and transferred to glass vials.

For high-performance liquid chromatography (HPLC) the vials were subjected to gentle nitrogen flow until complete dryness to evaporate the MeOH, followed by resuspension of the extract in 0.5 mL HPLC grade methanol and filtered (0.22 µm) into amber HPLC vials.

The extracts were analysed using HPLC system (Hitachi 5430 DAD, VWR, Carnaxide, PT) and recorded at 450nm with a diode array detector and with a Purosphere® STAR RP-18 edcapped column. A gradient program was used, with 9:1 (v/v) acetonitrile:water as solvent A (stationary phase) and ethyl acetate as solvent B (mobile phase) during 40 min at 27ºC. In the end, the pigment quantification was performed through calibration curves of standard pigments.

2.6. Data analysis

2.6.1.Growth model

To model microalgal growth kinetics, experimental data based on culture concentration (g L^{-1}) and DW determination were adjusted to a modified Verhulst logistic kinetic model (Verhulst et al. 1838). It is commonly used to describe microbial growth as a sinusoidal pattern (eq. 2), adjusting experimental data to a logistic curve.

$$\frac{dx(t)}{dt} = \mu_{DW,concentration}\, x(t)\ (1 - \frac{x(t)}{xmedium}) \quad (2)$$

Where $\mu_{DW,concentration}$ is the maximum growth rate of DW and culture concentration, *x(t)* represents the concentration of DW at time *t*, and x_{medium} represents the maximum of DW in the medium.

The parameters $\mu_{DW,concentration}$, *x(t),and* x_{medium} *and* are estimated fitting the data using Solver tool in Microsoft Excel. This tool employs a non-linear programming algorithm called GRG2, which optimizes the parameters by minimizing the sum of square residuals.

Once the parameters are estimated, productivity (P) can be calculated.

$$P = 0.9\, x_{medium} - 1.1\, x_0 \quad (3)$$

Equation 3 minimizes the effects of varying lag and stationary phases on the production rate by considering the time and concentration at which the lag and exponential phases ended—i.e, the time points when biomass concentration increased 10% from the initial value, $t(1.1\, x_0)$ and when 90% of maximum biomass concentration was reached $t(0.9\, x_{medium})$. For more details regarding the model see Ruiz et al. (2013).

2.6.2.Predictive models

For the development of predictive models, based on the simplex centroid augmented design (Figure 11), for each algae species, growth phase, and light intensities, were used 10 combinations derived from each POE experiment (see Annex 2). Using Stat-ease® software (Stat-Ease, Inc., Minneapolis, MN, USA) were obtained a visual representation of each model and statistical parameters, including the model equation, *f*-value, *p*-value, r^2, and the model's adequacy precision (see Annex 2). The model's equation found the optimal predicted ratio of red, green, and blue light for each algae species and growth phase at 200 and 500 µmol m^{-2} s^{-1}. Due to light intensity limitations of the light platforms used in this experiment, the models for 1000 µmol m^{-2} s^{-1} were not used for the development of the light regimes.

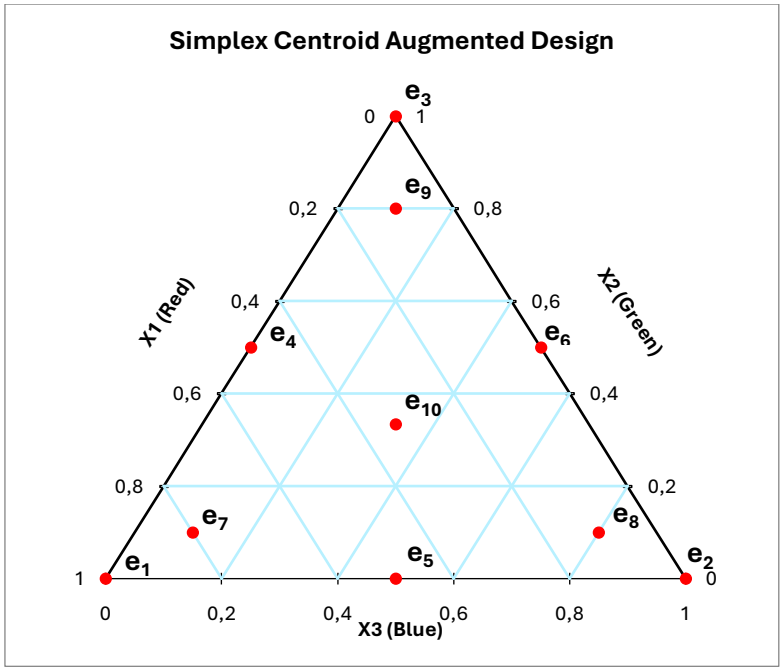

Figure 11 Visual representation of the simplex centroid augmented design used in the development of the predictor models (ternary contour plots). Each triangle edge (X1-X3) represents one light wavelength, and each red dot (e1-e10) represents one light combination.

3. Results

3.1. Photosynthesis – Irradiance curve

All culture concentrations (g L^{-1}) for *P. tricornutum* and *N. oceanica* were assessed using a successful linear correlation (r^2>0.97) between OD_{750} and dry weight (see Annex 4).

For *P. tricornutum* and *N. oceanica*, the transition from the photo-limited to the light-saturated phase occurred at a light intensity of 200 µmol s^{-1} m^{-2}. The maximum net photosynthetic rate was observed at 500 µmol s^{-1} m^{-2} for *N. oceanica*, beyond which the rate plateaued, indicating the onset of light saturation at 1000 µmol s^{-1} m^{-2}, whereas for *P. tricornutum*, at 5.0 g L^{-1} the maximum net photosynthesis rate was observed at 1000 µmol s^{-1} m^{-2} (Figure 12). These 3 light intensities were used in the POE trials with different combinations of red, green, and blue light wavelengths.

P. dioica exhibited negative net photosynthesis across all light intensities tested, suggesting that its respiration rate exceeded the photosynthetic rate, leading to a net loss in biomass. Figure 13 shows one of the photosynthetic oxygen evolutions of *P. dioica* used in the PI curve, at a concentration of 10 gFW L^{-1} under 50 µmol s^{-1} m^{-2} for 20 minutes. It shows a negative POE, in which the dissolved oxygen decreases from 110% to 45%. Due to the negative net photosynthesis rate, the POE trials with the various light combinations were not performed with *P. dioica*.

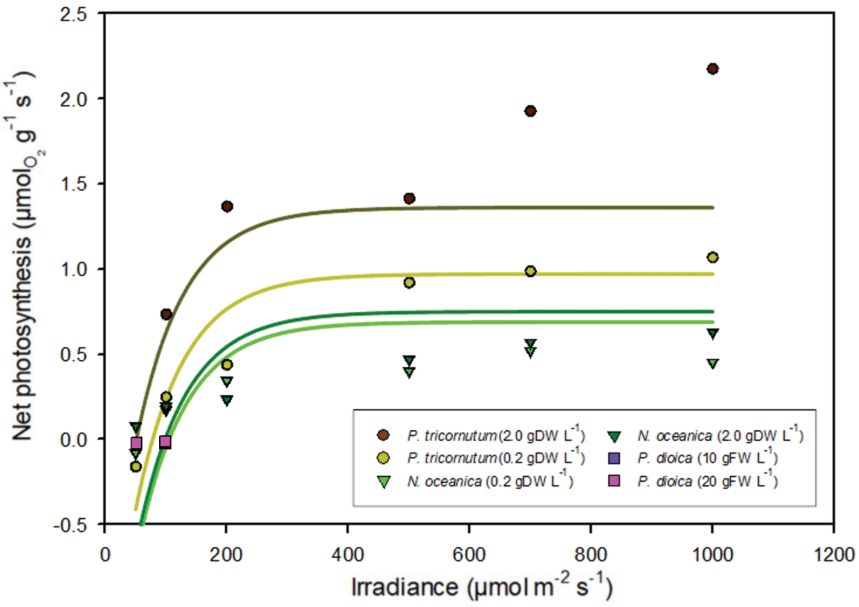

Figure 12 Photosyntehsis–Irradiance (PI) curve of *Phaeodactylum tricornutum*, *Nannochloropsis oceanica* (0.2 and 2.0 gDW L^{-1}), and *Porphyra dioica* (10 and 20 gFW L^{-1}), under a crescent increase of light intensity from 50 to 1000 µmol s^{-1} m^{-2}. All three species were adapted to continuous light intensity of 200 µmol s^{-1} m^{-2}. Solid lines are fitted to the PI curve data using a sigmoidal equation.

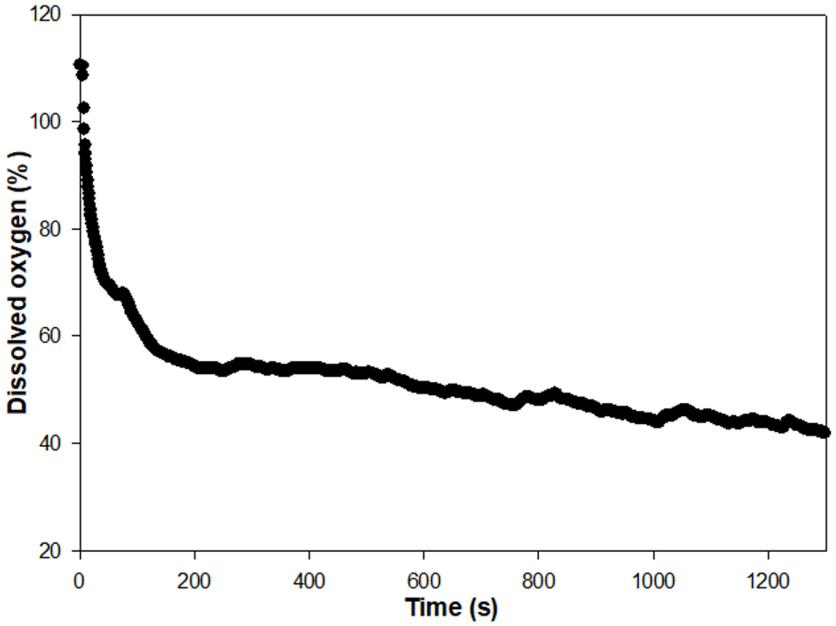

Figure 13 Photosynthetic oxygen evolution (POE) of *Porphyra dioica* at a concentration of 10 gFW L^{-1}, under 50 µmol s^{-1} m^{-2}. The graph plots time against DO2, %Sat (dissolved oxygen saturation).

3.2. POE trials and predictive models

The oxygen evolution trials were conducted to examine the impact of different light combinations on the photosynthetic oxygen evolution (POE) of *P. tricornutum* and *N. oceanica* under varying light intensities and biomass concentrations (Figure 14, Figure 15). For *Phaeodactylum tricornutum*, the ANOVA results revealed a negative correlation between blue light and POE (-0.36), a slight negative correlation with green light (-0.07), and a positive correlation with red light (0.412) (adjusted $r^2 = 0.30$) (Table 2). Similarly, for *Nannochloropsis oceanica*, the results showed a negative correlation of -0.33 for blue light, a minor negative correlation of -0.11 for green light, and a positive correlation of 0.43 for red light (adjusted $r^2 = 0.37$) (Table 2).

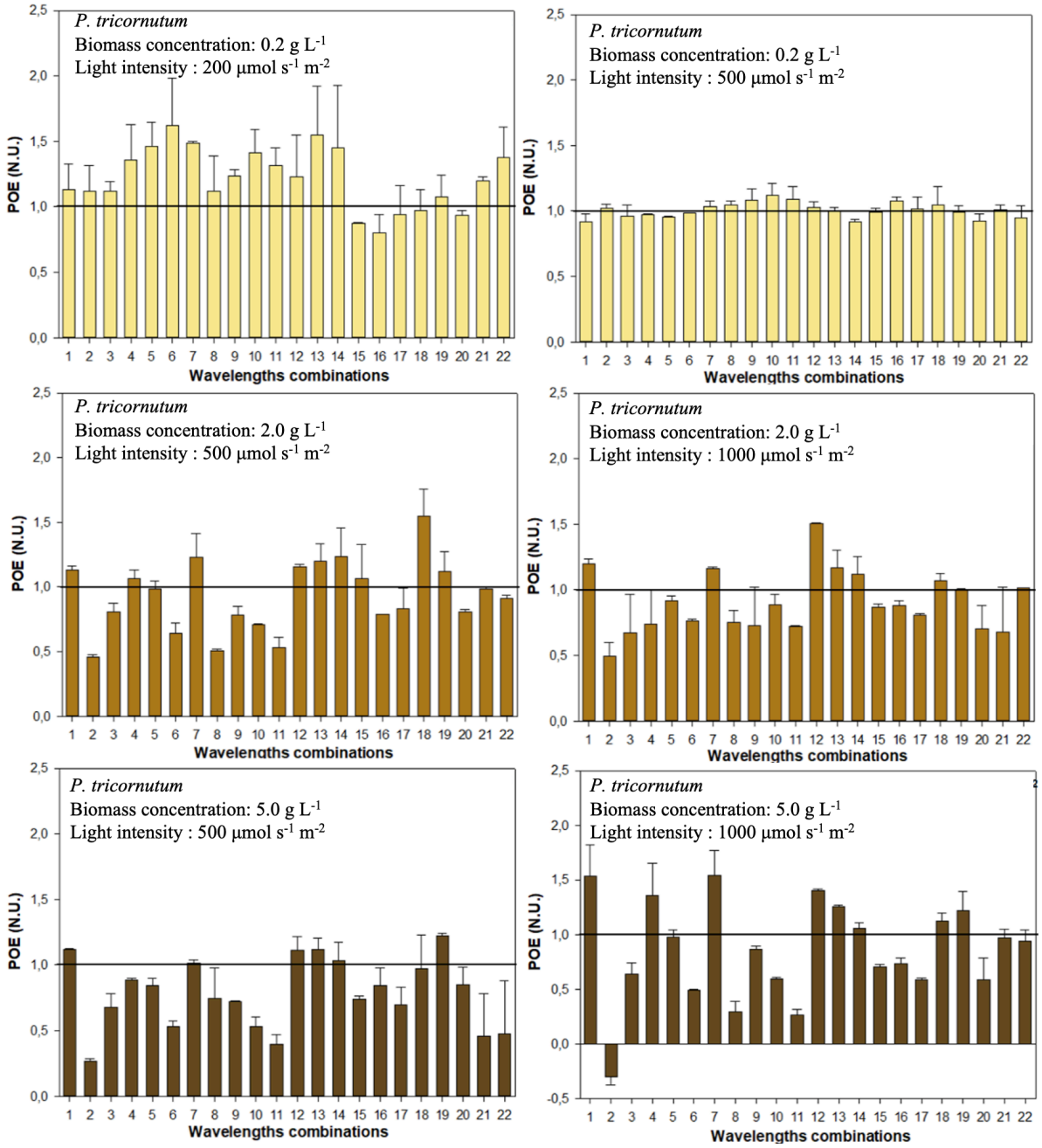

Figure 14 Photosynthetic oxygen evolution (POE) of *Phaeodactylum tricornutum* at concentrations of 0.2, 2.0, and 5.0 g L^{-1}. This resulted in 22 different light wavelength combinations of red, green, and blue (detailed in Table 1) at 3 light intensities: 200, 500, and 1000 µmol s^{-1} m^{-2}). The X-axis indicates each light wavelength combination was conducted in duplicate, and the Y-axis indicates the POE in normalized units (N.U.) compared to the control (N.U.=1) (warm white light). Data are shown as mean±SD, n=2.

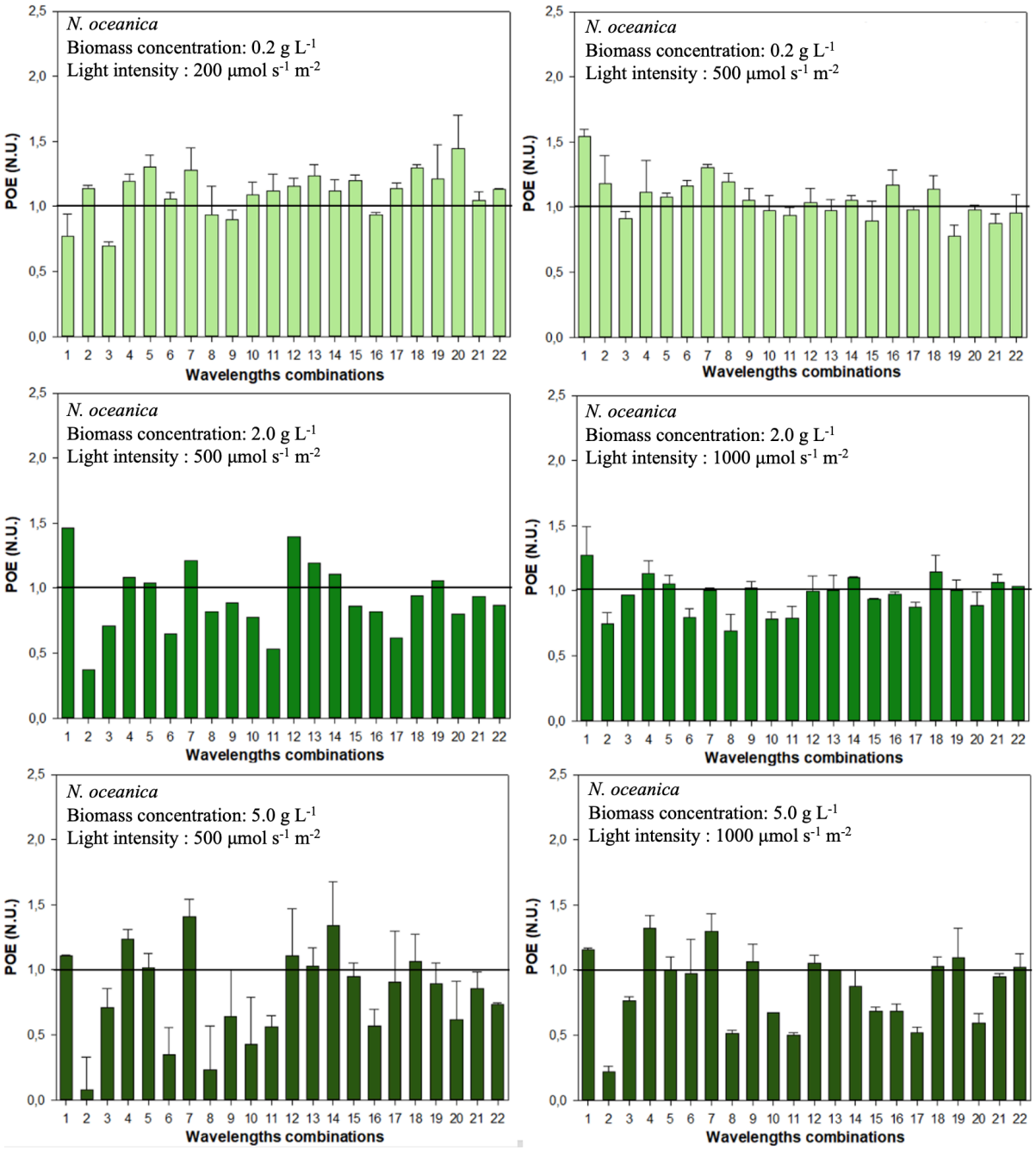

Figure 15 Photosynthetic oxygen evolution (POE) of *Nannochloropsis oceanica* at concentrations of 0.2, 2.0, and 5.0 g L^{-1}. This resulted in 22 different light wavelength combinations of red, green, and blue (detailed in Table 1) at 3 light intensities: 200, 500, and 1000 µmol s^{-1} m^{-2}. The X-axis indicates each light wavelength combination conducted in duplicate, and the Y-axis indicates the POE in normalized units (N.U.) compared to the control (N.U.=1) (warm white light). Data are shown as mean±SD, n=2.

Table 2 Correlation matrix showing the relationships between different light wavelengths (red, green, blue) and photosynthetic oxygen evolution (POE) in *Phaeodactylum tricornutum* and *Nannochloropsis oceanica*. Positive values indicate a direct correlation, while negative values indicate an inverse correlation.

	P. tricornutum				*N. oceanica*			
	Red	**Green**	**Blue**	**POE**	**Red**	**Green**	**Blue**	**POE**
Red	1	-0.48	-0.56	0.42	1	-0.48	-0.56	0.43
Green	-0.48	1	-0.46	-0.07	-0.48	1	-0.46	-0.11
Blue	-0.56	-0.46	1	-0.36	-0.56	-0.46	1	-0.33
POE	0.42	-0.07	-0.36	1	0.43	-0.11	-0.33	1

Twelve predictive models were developed to describe the POE experimental data (Figure 14, Figure 15), which were named as MD*n*, in which the *n* denotes the model number. Notably, statistically significant models (p<0,05, Figure 16, see annex 2) were obtained for *P. tricornutum* cultures with biomass concentrations of 2.0 g L^{-1} and light intensities of 500 µmol s^{-1} m^{-2} (MD1) and 2.0 g L^{-1} (MD2) and biomass concentrations of 5.0 g L^{-1} and light intensities of 500 µmol s^{-1} m^{-2} (MD3) and 1000 µmol s^{-1} m^{-2} (MD4). The best photosynthetic performance for *P. tricornutum* cultures at 2.0 and 5.0 g L^{-1} was reached under 100% red light when 500 µmol s^{-1} m^{-2} was used (MD1 and MD3). At a higher light intensity, 1000 µmol s^{-1} m^{-2}, the best photosynthetic performance for *P. tricornutum* at both 2.0 and 5.0 g L^{-1} was also achieved with 100 % red light (MD2 and MD4). The model predicting the best light combination for a biomass concentration at 0.2 g L^{-1} under 200 or 500 µmol s^{-1} m^{-2} was not statistically significant (p>0.05).

For *N. oceanica*, statistically significant models were obtained (p<0,05, Figure 16 see annex 2) of 0.2 g L^{-1} biomass and light intensity of 500 µmol s^{-1} m^{-2} (MD5), of 2.0 g L^{-1} under 500 and 1000 µmol s^{-1} m^{-2} (MD6 and MD7), and lastly for biomass of 5.0 g L^{-1} at light intensities of 500 and 1000 µmol s^{-1} m^{-2} (MD8 and MD9). MD5 and MD6 reveal that for *N. oceanica* cultures at 0.2 and 2.0 g L^{-1} the best photosynthetic performance was achieved with 100% red light and 500 µmol s^{-1} m^{-2}. MD7 suggested a higher photosynthetic performance when 100% red light and 1000 µmol s^{-1} m^{-2} were used. At higher concentrations (5.0 g L^{-1}), under 500 µmol s^{-1} m^{-2}, 75% red and 25% green light showed best photosynthetic performance whereas under 1000 µmol s^{-1} m^{-2} the optimal ratio is 70% red and 30% green light. The model predicting the best light combinations for 0.2 g L^{-1} under 200 µmol s^{-1} m^{-2} was not statistically significant (p>0.05).

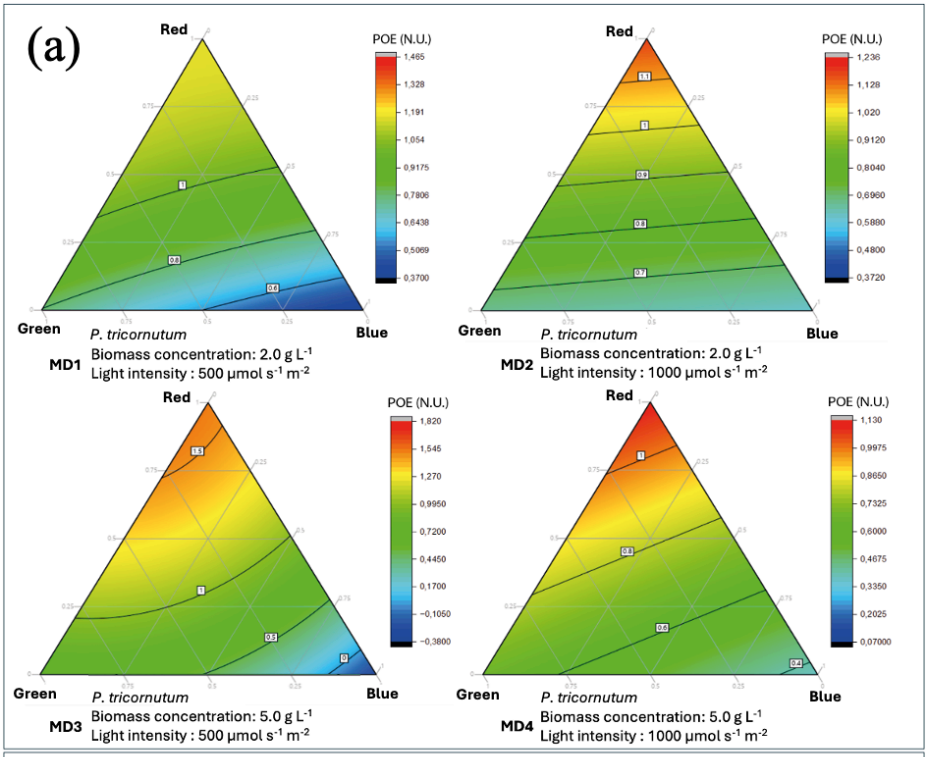
(a)
Red
Green
Blue
POE (N.U.)
P. tricornutum
MD1
Biomass concentration: 2.0 g L-1
Light intensity : 500 µmol s-1 m-2
MD2
Biomass concentration: 2.0 g L-1
Light intensity : 1000 µmol s-1 m-2
MD3
Biomass concentration: 5.0 g L-1
Light intensity : 500 µmol s-1 m-2
MD4
Biomass concentration: 5.0 g L-1
Light intensity : 1000 µmol s-1 m-2

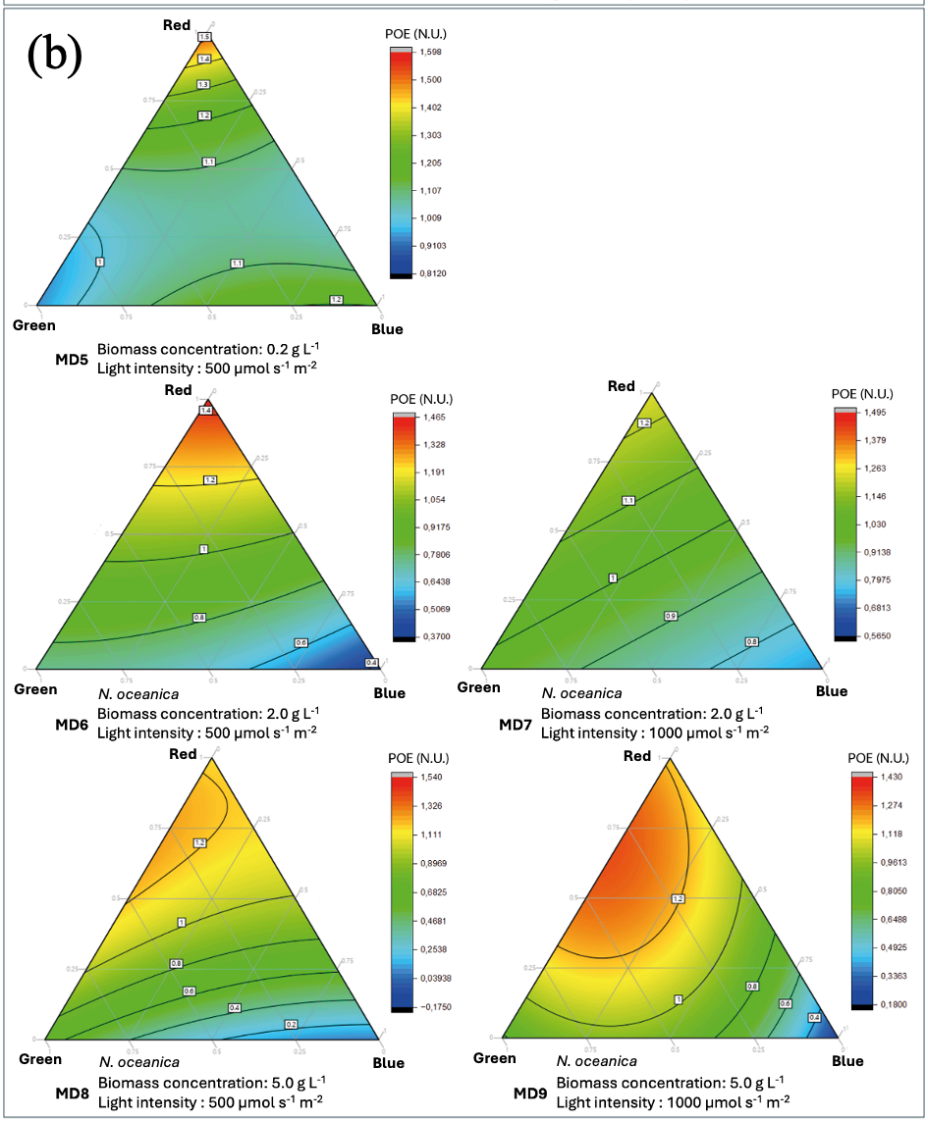
(b)
Red
Green
Blue
POE (N.U.)
MD5
Biomass concentration: 0.2 g L-1
Light intensity : 500 µmol s-1 m-2
N. oceanica
MD6
Biomass concentration: 2.0 g L-1
Light intensity : 500 µmol s-1 m-2
MD7
Biomass concentration: 2.0 g L-1
Light intensity : 1000 µmol s-1 m-2
MD8
Biomass concentration: 5.0 g L-1
Light intensity : 500 µmol s-1 m-2
MD9
Biomass concentration: 5.0 g L-1
Light intensity : 1000 µmol s-1 m-2

Figure 16 Ternary contour plots of the predictive models for *Phaeodactylum tricornutum* (a) and *Nannochloropsis oceanica* (b). Equations and statistical analysis are provided in Annex 2. Each ternary illustrates the predictive model of photosynthetic oxygen evolution (POE) in normalized units (compared with the warm-white light control) according to various ratios of red (620 nm), green (530 nm), and blue (450 nm) light wavelengths.

3.3. Light regime validation

To validate the most promising light regimes at a given growth stage, light regimes were estimated as most promising for batch cultivation according to the predictive models (section 3.2). For *P. tricornutum* during lag phase (0.2 – 2.0 g L^{-1}), control warm white at a light intensity of 500 µmol s^{-1} m^{-2} was applied; as the culture entered the exponential phase (2.0 – 5.0 g L^{-1}), the light setup shifted to 100% red light at the same light intensity of 500 µmol s^{-1} m^{-2}; during late exponential phase (past 5.0 g L^{-1}) 100% red under 500 µmol s^{-1} m^{-2} continued to be used (Figure 17). The duplicates under the developed light regime exhibited average batch cultivation productivity of 0.88±0.02 g L^{-1} day^{-1}, and maximum biomass concentration of 6.76±0.30 g L^{-1}, which was not significantly different to the control cultures under warm white light (0.67±0.07 g L^{-1} day^{-1}, and 6.25±0.02 g L^{-1}, respectively; $p<0.05$).

For *N. oceanica* during lag phase (0.2 – 2.0 g L^{-1}), 100% red light at a light intensity of 500 µmol s^{-1} m^{-2} was used; during exponential phase (2.0 – 5.0 g L^{-1}) the same ratio of 100% red light and light intensity 500 µmol s^{-1} m^{-2} was maintained; during late exponential phase (past 5.0 g L^{-1}) the light was adjusted to 75% red and 25% green light under 500 µmol s^{-1} m^{-2} (Figure 18). The duplicates under the light regime showed batch cultivation productivity of 0.49±0.01 g L^{-1} day^{-1} and maximum biomass concentration of 6.04±0.48 g L^{-1} while the control cultures under warm white light had values of 0.46±0.01 g L^{-1} day^{-1} and 5.41±0.15 g L^{-1}, respectively. Nevertheless, the results of statistical analysis did not indicate any statistically significant differences between the light regime and the control ($p>0.05$).

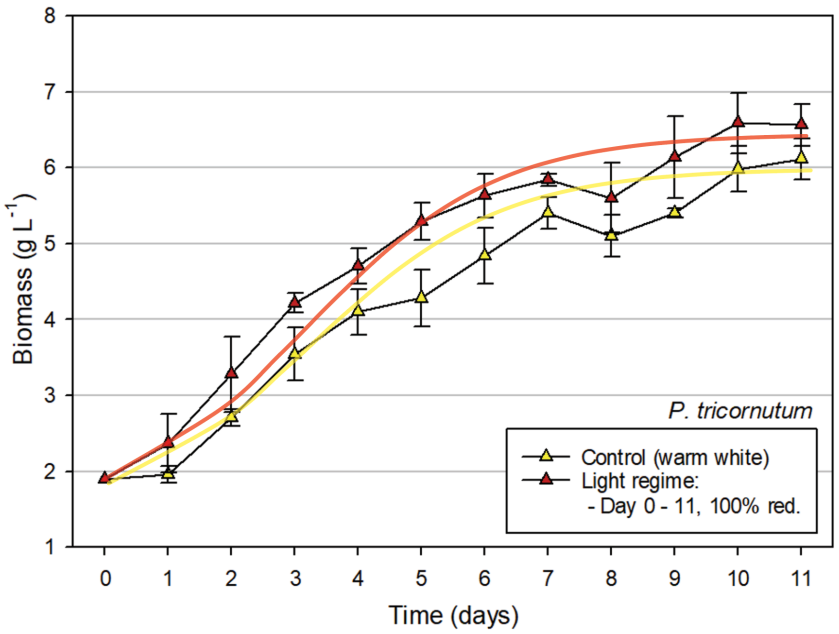

Figure 17 Comparing growth curve of control warm-white light conditions with light regimes under 500 µmol s^{-1} m^{-2} light intensity for *P.tricornutum*. The light regime started at 2.0 g L^{-1} under 100% red light until late exponential phase (MD1 and MD3 from Figure 16). Light solid lines are fitted to the growth data using sigmoidal growth model according to Ruiz et al. 2013. Data are shown as mean±SD, n=2.

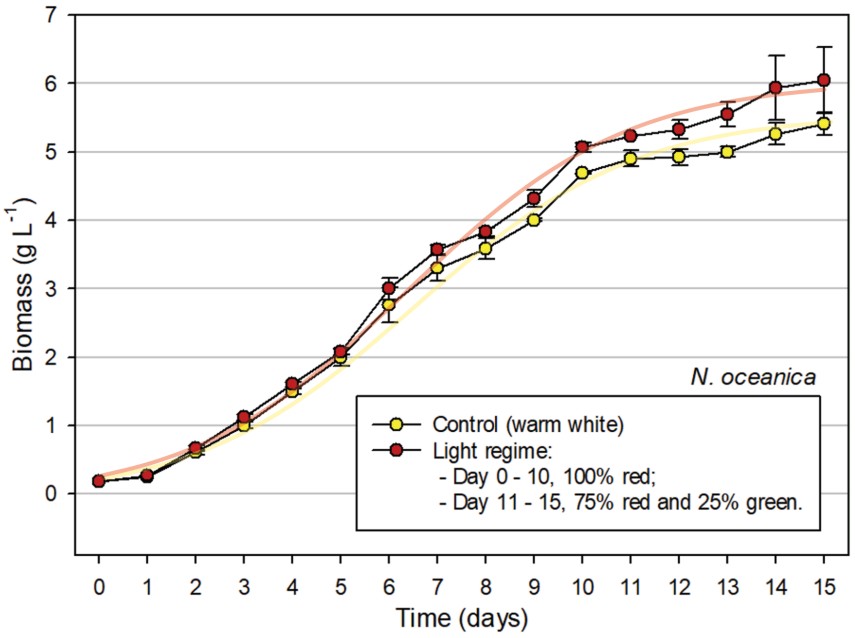

Figure 18 Comparing growth curve of control warm-white light conditions with light regimes under 500 µmol s^{-1} m^{-2} light intensity for *N. oceanica*. The light regime started at 0.2 g L^{-1} under 100% red light until 5.0 g L^{-1}, whereas the light was adjusted to 25% green and 75% red light (MD5, MD6 and MD8 from Figure 16). Light solid lines are fitted to the growth data using sigmoidal growth model according to Ruiz et al. 2013. Data are shown as mean±SD, n=2.

3.4. Biochemical parameters

3.4.1. Pigments

The pigment profile of *P. tricornutum* was dominated by pigment fucoxanthin ranging from 2.61 ± 2.47 to 5.8 ± 0.18 mg g^{-1}, followed by lower amounts of chlorophyll-*a* (1.17 ± 0.15 to 0.37 ± 0.29 mg g^{-1} (Table 3). Effects of light treatments on these pigments were not significant for *P. tricornutum* among the tested light regime and the control warm white light (p >0.05). The pigment profile of *N. oceanica* had similar amount of pigment zeaxanthin and chlorophyll *a*, ranging from 0.28 ± 0.07 to 0.52 ± 0.24 mg g^{-1} and 0.26 ± 0.07 to 0.49 ± 0.19 mg g^{-1}, respectively (Table 3). In the control condition violaxanthin was detected at 0.38 ± 0.15 mg g^{-1} of violaxanthin while in the light regime treatment, its concentration was below the detectable limit. Effect of light treatments on zeaxanthin and chlorophyll-a were not significant for *N. oceanica* among the tested light regime and the control warm white light (p>0.05).

Table 3 Carotenoids and chlorophyll contents from the light regime experiment for *Phaeodactylum tricornutum* and *Nannochloropsis oceanica*.

	Pigments (mg gDW^{-1})									
	Fucoxanthin	**Neoxanthin**	**Violaxanthin**	**Lutein**	**Zeaxanthin**	***a*-Carotene**	***b*-Carotene**	**Chlorophyll *a***	**Chlorophyll *b***	**Chlorophyll *c***
Phaeodactylum tricornutum (control)	5.80 ± 0.18	n.d.	n.d.	n.d.	n.d.	0.3 ± 0.07	n.d.	1.17 ± 0.15	n.d.	n.d.
Phaeodactylum tricornutum (light regime)	2.61 ± 2.47	n.d.	n.d.	n.d.	n.d.	n.d.	n.d.	0.37 ± 0.29	n.d.	n.d.
Nannochloropsis oceanica (control)	n.d.	n.d.	0.38 ± 0.15	n.d.	0.28 ± 0.07	n.d.	n.d.	0.26 ± 0.07	n.d.	n.d.
Nannochloropsis oceanica (light regime)	n.d.	n.d.	n.d.	n.d.	0.52 ± 0.24	n.d.	n.d.	0.49 ± 0.19	n.d.	n.d.

4. Discussion

4.1. Photosynthesis – irradiance curve

At low light intensities for *P. tricornutum*, below 200 µmol s^{-1} m^{-2}, the curve shows gradual increase in the net photosynthesis for 0.2 and 2.0 g L^{-1}. At both concentrations the slope is similar suggesting that this is where light is limited, and net photosynthesis can increase as long as light intensity also increases independently of cell concentration.

For *P. tricornutum,* as light intensities increase beyond 500 µmol s^{-1} m^{-2}, at a concentration of 0.2 g L^{-1} the photosynthesis rates start to plateau, suggesting that the photosynthetic apparatus is becoming saturated, meaning that the increase in light intensity stops being the limiting factor (Tyystjärvi, 2013). On the other hand, at concentration of 2.0 g L^{-1} the net photosynthesis keeps increasing until 1000 µmol s^{-1} m^{-2} not showing signs of photoinhibition.

For *N. oceanica*, at a low biomass concentration, 0.2 g L^{-1}, the result was similar with *P. tricornutum*, in which at 500 µmol s^{-1} m^{-2}, the net photosynthesis started to plateau, suggesting that light ceased to be the limiting factor for the net photosynthesis increase (Vonshak et al., 2020).

The discrepancy in the results of high concentration culture, 2.0 g L^{-1}, P-I curve between *P. tricornutum* and *N. oceanica* could be attributed to two main factors: (1) *P. tricornutum* being more resistant to high light intensities, or (2) *N. oceanica* culture could have been experiencing some form of stress leading to low net photosynthesis. This is further supported by other studies, which report photosynthesis rate for *N. oceanica* that are comparable to those observed in *P. tricornutum* under similar conditions (Schulze et al. 2020).

The increase in cell concentration from 0.2 to 2.0 g L^{-1} results in a significant reduction in light penetration due to light absorption and scattering by the cells at the periphery layer of the photosynthetic chamber, originating larger dark zones, described by the Beer-Lambert law (Richmond, 2004; Sukenik et al. 1993). For *P. tricornutum*, the increase in net photosynthesis at high concentration, 2.0 g L^{-1}, and light intensities higher than 1000 µmol s^{-1} m^{-2}, could indicate that the duration of the circulation of cells in the medium between the light zone (high light intensity) and the dark zone (low light intensity) in the present setup, was enough to repair the PSII mechanism after photoinhibition due to excessive light intensity and the time in the dark zone is not long enough to inhibit the repair of PSII, as it need light intensity to be repaired (Tyystjärvi, 2013).

Regarding *P. dioica*, both concentrations, 10 and 20 gFW L^{-1}, experienced negative photosynthetic oxygen evolution, regardless of the light intensity. These results suggest that the photorespiration rate of this algae was higher than the photosynthesis rate, hence the decrease in oxygen concentration. Also, *P. dioica* did not grow in the batch cultivation aside from the experiment, meaning that during the POEs this alga was already stressed. During cultivation maintenance, a discolouration occurred. This stress could be originated during shipping, from Aveiro to Faro, or by environmental factors such as nutrient deficiency or contamination (Amano and Noda, 19987). Because of these results, *P. dioica* was removed from the POE trials and posterior light regime validation experiment. Other authors observed for this species electron transport rates ranging from 2 to 5 μmol electrons m^{-2} s^{-1} under a range of 200 to 1000 μmol light intensity, which can be converted in 0.5 to 1.3 $umol_{O2}$ g^{-1} s^{-1}, values slightly lower than the ones shown in *P. tricornutum* and *N.oceanica*, however in the present study only respiration could be observed, indicating that the culture conditions could not support growth of this species (Tala and Chow, 2014).

4.2. Photosynthesis oxygen evolution trials

While this study aimed to identify significant variations in POE under different light conditions, it is important to note that the statistical analyses, including Dunnett's and Tukey's tests, did not reveal any statistically significant differences (p<0.05) among the 22 combinations tested in every chart. Nevertheless, the ANOVA results, indicate varying relationships between the experimental variables (biomass, red, green, and blue light) and the POE response (N.U.). The strongest positive correlation is observed between POE results. and red light for both species, suggesting that higher red-light ratios enhance photosynthesis efficiency. In contrast, blue light shows a moderate negative correlation, implying an inhibitory effect of blue light on photosynthetic oxygen response. There is minimal correlation between POE and green light (-0.066), reflecting its limited role in influencing photosynthesis. Overall, the results highlight the critical role of light quality and intensity in modulating photosynthetic efficiency in this microalgae species, with red light (620 nm, low absorption) having a positive effect and blue light (450nm, highly absorption) contributing negatively. Additionally, POE rate of both microalgae was influenced by light intensity and biomass, with higher light intensities and greater microalgae concentrations generally leading to an increase in photosynthetic oxygen levels. An increase in light intensity increases the oxygen production rate, but also causes inhibition of the PSII over time. Additionally, although higher microalgae

biomass is expected to produce more oxygen, it is not always true as an increase in biomass also increases the auto shading effect, reducing the light transmittance, and thus causing inhibition of the oxygen production (Blair et al., 2014; Kang et al., 2019).

During the POE trials it was possible to visually notice the impact of different wavelengths on the quantity of photons traveling through the algal culture, evidencing the dark-light zone ratios in each green (530 nm), blue (450 nm) and red (620 nm) light at 500 μmol s^{-1} m^{-2} (see Annex 1). In both algae, the difference between POE in light wavelength combinations and control increased with concentration (0.2, 2.0, 5.0 g L^{-1}) because the more concentrated the culture the more amplified is the result of the dark and light zones in the photosynthetic chamber. This may have been the reason, why predictor models for 0.2 g L^{-1} at 200 μmol s^{-1} m^{-2} for both microalgae species did not show statistical significance. Interestingly, the in-vivo absorption spectrum showed peaks at wavelengths of the tested blue light (Figure 10) and lowest – even negative- photosynthesis rates were observed when 500 μmol s^{-1} m^{-2} and 5.0 g L^{-1} were used. This may be explained as at high culture concentrations, the cells in the culture are mainly in the dark zone due to low light penetration depths and thus adapted to low light conditions. When these cells travel to the light zone, they may get inhibited, and respiration rates become higher than oxygen evolution rates (Tyystjärvi, 2013).

On the other hand, red light wavelengths were not as strong absorbed compared to the blue ones (see in-vivo absorption spectrum), resulting in the highest POE result compared to green and blue. At concentrate cultures, red light showed the highest ratio of light zone in the experiment compared with dark zone (see Annex 1). This may suggest that the traveling period of cells in the small dark zone was sufficiently long to repair PSII damage.

The reason *P. tricornutum* and *N. oceanica* have similar predictive models for all light intensities and biomass concentrations may be because both have present chlorophyll-a (that absorbs primarily in the red 660 nm and blue 430 nm regions) and highly rely on that pigment for photosynthesis, although they have different accessory pigments, such as fucoxanthin in *P. tricornutum* and violaxanthin in *N. oceanica* (Conceição et al.2020; Liu et al. 2023).

Although several studies tested the effect of light quantity and quality on the oxygen production rate of microalgae, there are no clear mechanisms or conclusive results that correlate the effect of light quality and quantity with culture concentration, which showed in this study to be a crucial parameter that affect the amount of light and dark zone in the culture, and consequently the amount of time cells are fully exposed to light (Yan et al., 2013; Kang et al., 2018; Blair et al., 2014; Johkan et al., 2012)

4.3. Light regime validation

Although red light was predicted by the model to have the best photosynthetic efficiency and was used in the light regime validations, its effect on the biochemical analysis of pigments showed no significant difference. This is mainly because, this LEDs emitted at the lower end of the red-wavelength rage (620 nm), which is not at the peak absorption wavelength of pigments (660 nm) (Kuczyńska et al. 2015; Possa et al. 2017). However, it was sufficient to stimulate PSII and penetrate the culture, allowing a much larger number of cells to photosynthesize compared to the control warm white light.

Despite the higher productivity and maximum biomass concentration values observed under the light regime condition, more trials are required to determine whether this light regime consistently leads to increased productivity and maximum biomass concentration. It is suggested that using specific narrow wavelength ranges (e.g., 620 nm) may be more energy-efficient than using broad wavelength ranges at the same light intensity, as broad wavelength ranges include photons at non-optimal wavelengths for photosynthesis. For instance, studies have shown that plants exposed to narrow-band LEDs exhibit higher growth rates and biomass accumulation while consuming less electrical energy (Miao et al., 2016).

Regarding pigment concentration (Table 3), the values did not align with the findings reported in the literature (Solovchenko et al., 2014; Conceição et al., 2020), suggesting potential methodological errors. These discrepancies could be due to improper calibration of chromatogram wavelength peaks for each pigment in HPLC, resulting in undetected compounds, or handling errors during pellet measurements after freeze-drying, thus preventing further discussion.

4.4. AlgaeLum

A novel light system was developed (see Annex 5). During AlgaeLum version 1, certain issues were noted and subsequently improved. The Schott flask containing the algae culture would overheat (6ºC above room temperature) due to continuous LED exposure and lack of aeration. Additionally, the LED RGB controller only allowed a limited number of predefined light combinations, and the LED strip was vulnerable to potential spillage during cultivation.

AlgaeLum version 2 addresses all the issues from version 1. It maintains room temperature more effectively (max. +2ºC above ambient temperature at light intensity of 1000 μmol s^{-1} m^{-2}), protects LEDs from possible spills, and introduces a new LED controller that allows more

customizable light quality and intensity combinations. The introduction of the customizable AlgaeLum autoclavable lid opens new possibilities for future applications using the standard Schott flask. This lid allows full control of temperature through water-water temperature exchanges, temperature and pH measurements, and multiple gas and medium inputs and outputs.

Future iterations of AlgaeLum could integrate microcontrollers, aiming for fully automated control over abiotic parameters such as pH, temperature, aeration, lighting, and turbidity. This would contribute to further innovations in the field while maintaining low production costs.

The primary motivation behind this creative effort was to simplify and accelerate algae-based light effect experiments, enhance the capabilities of 3D printing in algae research, and provide new, more affordable solutions compared to the lab-scale photobioreactors currently available on the market.

5. Conclusion

Light quality and intensity were found to influence the quantity of photons passing through an algal culture, impacting the photosynthetic oxygen evolution rates of *P. tricornutum* and *N. oceanica*. The developed predictive models showed an increase in photosynthesis efficiency when low-absorbed red light (620 nm) was used for both algae. When applying the predicted light regimes to a batch culture with a longer light path, no significant differences were found in biomass productivity, maximum biomass concentration, or pigment contents. This suggests that while low-absorbed wavelengths improve photosynthesis efficiency, they do not necessarily translate into enhanced growth or pigment synthesis in batch cultures using longer light paths.

AlgaeLum successfully delivered the required light quantity and quality throughout all validation experiments, proving to be a promising platform for conducting light condition experiments in microalgae research. Its performance in this study, including light homogeneity delivery, practicability, and ease of use, outperforming traditional self-constructed light setups. Further experiments with a higher number of replicates are necessary to better understand the long-term effects of low-absorbed wavelengths on microalgal growth, productivity, and pigment accumulation. If proven effective, the energy efficiency of using a narrow range of wavelengths may reduce operational costs, extend the lifespan of the LEDs, and reduce the

need for cooling. This work contributes to the development of energy-efficient light solutions for microalgal cultivation.

6. References

Al-Dailami, A., Ahmad, I., & Goto, M. (2022). Potential of photobioreactors (PBRs) in cultivation of microalgae. *J. Adv. Res. Appl. Sci. Eng. Technol.*, 27(1), 32–44.

Amano, H., & Noda, H. (1987). Effect of nitrogenous fertilizers on the recovery of discoloured fronds of *Porphyra yezoenisis*. *Bot. Mar.*, 30, 467-473.

Amaral, M., Loures, C., Naves, F., Samanamud, G., Silva, M., & Prata, A. (2021). Microalgae cultivation in photobioreactors aiming at biodiesel production. *Renew. Energy, 169*, 587-598.

Angelov, A., & Lecheva, M. (2023). Impact of light wavelength on the performance of algae-assisted microbial fuel cell. *J. Appl. Phycol.*, 35, 789-800.

Berberoglu, H., Gomez, P. S., & Pilon, L. (2008). Radiation characteristics of microalgae for photobioreactors. *J. Quant. Spectrosc. Radiat. Transfer*, 109(14), 2120–2130.

Blair, M. F., Kokabian, B., & Gude, V. G. (2014). Light and growth medium effect on *Chlorella vulgaris* biomass production. *J. Environ. Chem. Eng.*, 2(1), 665–674.

Cañedo, J. C. G., & Lizárraga, G. L. L. (2016). Considerations for photobioreactor design and operation for mass cultivation of microalgae. *InTech*., 55-74.

Carneiro, M., Cicchi, B., Maia, I. B., Pereira, H., Chini Zittelli, G., Varela, J., Malcata, F. X., & Torzillo, G. (2020). Effect of temperature on growth, photosynthesis, and biochemical composition of *Nannochloropsis oceanica*, grown outdoors in tubular photobioreactors. *Algal Res.*, 49, 101923.

Carreto, J. I., & Carignan, M. O. (2011). Mycosporine-like amino acids: Relevant secondary metabolites. Chemical and ecological aspects in marine environments. *Mar. Drugs*. 21(3), 387-446.

Chang, J.-S., Show, P.-L., Ling, T.-C., Chen, C.-Y., Ho, S.-H., Tan, C.-H., & Phong, W.-N. (2017). Photobioreactors. In *Current Developments in Biotechnology and Bioengineering* (pp. 313–352). Elsevier.

Chen CY, Yeh KL, Aisyah R, Lee DJ, Chang JS. (2011) Cultivation, photobioreactor design and harvesting of microalgae for biodiesel production: a critical review. *Bioresour. Technol.* 102(1), 71-81.

Chinnasamy, S., Rao, P. H., Bhaskar, S., Rengasamy, R., & Singh, M. (2012). *Algae*. A Novel Biomass Feedstock for Biofuels.

Cho, J., Park, J. H., Kim, J. K., & Schubert, E. F. (2017). White light-emitting diodes: history, progress, and future. *Laser Photonics Rev.*, 11(2).

Conceição, D., Lopes, R. G., Derner, R. B., Cella, H., do Carmo, A. P. B., Montes D'Oca, M. G., Petersen, R., Passos, M. F., Vargas, J. V. C., Galli-Terasawa, L. V., & Kava, V. (2020). The effect of light intensity on the production and accumulation of pigments and fatty acids in *Phaeodactylum tricornutum*. *J. Appl. Phycol.*, 32, 1017–1025.

Converti, A., Casazza, A. A., Ortiz, E. Y., Perego, P., & Borghi, M. D. (2009). Effect of light on biomass and metabolite production in microalgae cultures. *Biochem. Eng. J.*, 43, 121–129.

Cornet, J. F., Dussap, C. G., & Gros, J. B. (1994). Conversion of radiant light energy in photobioreactors. *AIChE J.*, 40(6), 1055–1066.

Christaki, E., Bonos, E., Giannenas, I., & Florou-Paneri, P. (2013). Functional properties of carotenoids originating from algae. *J. Sci. Food Agric.*, 93(1), 5-11.

Cuaresma, M., Janssen, M., Vílchez, C., & Wijffels, R. (2011). Horizontal or vertical photobioreactors? How to improve microalgae photosynthetic efficiency. *Bioresour. Technol.*, 102(8), 5129–5137.

Darvehei, P., Bahri, P. A., & Moheimani, N. R. (2018). Model development for the growth of microalgae: A review. *Renew. Sustain. Energy Rev.*, 97, 233–258.

Data Bridge Market Research. (2023). *Microalgae market share, scope, value & trends to 2030*. Retrieved [08-2024], from https://www.databridgemarketresearch.com/reports/global-microalgae-market.

Dong, M., Zhang, Y., Yu, Q., Liu, Q., Zhou, X., & Jin, C. (2023). Regulation of light quality on lipid production, biodiesel quality, and nutritional quality of *Phaeodactylum tricornutum*. *Aquac. Int.*, 31, 1231–1251.

Duarte, B., Feijão, E., Goessling, J. W., Caçador, I., & Matos, A. R. (2021). Pigment and fatty acid production under different light qualities in the diatom *Phaeodactylum tricornutum*. *Applied Sciences*, 11(6), 2550.

Fernandez-Marchante, C. M., Asensio, Y., Lobato, J., Villaseñor, J., Cañizares, P., & Rodrigo, M. A. (2018). Influence of hydraulic retention time and carbon loading rate on the production of algae. *J. Biotechnol.*, 282, 70–79.

Future Market Insights. (2023). Microalgae market size, share & forecast report by 2033. Retrieved [08-2024], from www.futuremarketinsights.com/reports/microalgae-market.

Glazer, A. N. (1989). Light guides. Directional energy transfer in a photosynthetic antenna. *J. Biol. Chem.* 5, 264(1),1-4.

Glemser, M., Heining, M., Schmidt, J., Becker, A., Garbe, D., Buchholz, R., & Brück, T. (2015). Application of light-emitting diodes (LEDs) in cultivation of phototrophic microalgae: Current state and perspectives. *Appl. Microbiol. Biotechnol.*, 100(3), 1077–1088.

Haris, N., Manan, H., Jusoh, M., Khatoon, H., Katayama, T., & Kasan, N. A. (2022). Effect of different salinity on the growth performance and proximate composition of isolated indigenous microalgae species. *Aquacult. Rep.*, 22, 100925.

Heining, M., & Buchholz, R. (2015). Photobioreactors with internal illumination – A survey and comparison. *Biotechnol. J.*, 10(8), 1131–1137.

Hong, Y., Yang, L., You, X., et al. (2023). Effects of light quality on microalgae cultivation: Bibliometric analysis, mini-review, and regulation approaches. *Environ. Sci. Pollut. Res.*

Kang, D., Kim, K., Heo, T., Kwon, G., Lim, C., & Park, J. (2019). Inhibition of photosynthetic activity in wastewater-borne microalgal–bacterial consortia under various light conditions. *Sustainability*, 11(10), 2951.

Kang, D., Kim, K., Jang, Y., Moon, H., Ju, D., & Jahng, D. (2018). Nutrient removal and community structure of wastewater-borne algal-bacterial consortia grown in raw wastewater with various wavelengths of light. *Int. Biodeterior. Biodegrad.*, 126, 10–20.

Katsuda, T., Arimoto, T., Igarashi, K., Azuma, M., Kato, J., Takakuwa, S., & Ooshima, H. (2000). Light intensity distribution in the externally illuminated cylindrical photo-bioreactor and its application to hydrogen production by *Rhodobacter capsulatus*. *Biochem. Eng. J.*, 5(2), 157–164.

Khoo, K. S., Chew, K. W., Yew, G. Y., Leong, W. H., Chai, Y. H., Show, P. L., & Chen, W. H. (2020). Recent advances in downstream processing of microalgae lipid recovery for biofuel production. *Bioresour. Technol.*, 304, 122996.

Kim, S., Sunwoo, I., Hong, H., Che, C. A., Jeong, G. T., & Kim, S. K. (2019). Lipid and unsaturated fatty acid productions from three microalgae using nitrate and light-emitting diodes with complementary LED wavelength in a two-phase culture system. *Bioprocess Biosyst. Eng.*, 42, 203–210.

Kirk, J. T. O. (1994). Light and photosynthesis in aquatic ecosystems. Cambridge University Press. 509.

Kuczyńska, P., Jemiola-Rzeminska, M., & Strzałka, K. (2015). Photosynthetic pigments in diatoms. *Mar. Drugs*, 13, 5847–5881.

Kumar, K., Ergas, S., Yuan, X., Sahu, A., Zhang, Q., Dewulf, J., Malcata, F. X., & Van Langenhove, H. (2010). Enhanced CO_2 fixation and biofuel production via microalgae: Recent developments and future directions. *Trends Biotechnol.*, 28, 371–380.

Lepetit, B., Volke, D., Gilbert, M., Wilhelm, C., & Goss, R. (2010). Evidence for the existence of one antenna-associated, lipid-dissolved and two protein-bound pools of diadinoxanthin cycle pigments in *Phaeodactylum tricornutum*. *Plant Physiol.*, 154(3), 1828–1839.

Liu, M., Ding, W., Pan, Y., et al. (2023). Zeaxanthin epoxidase is involved in the carotenoid biosynthesis and light-dependent growth of the marine alga *Nannochloropsis oceanica*. *Biotechnol. Biofuels*, 16, 74.

Liu, X., & van Iersel, M. W. (2021). Photosynthetic physiology of blue, green, and red light: Light intensity effects and underlying mechanisms. *Front. Plant Sci.*, 12, 619987.

López, M. A., González, M. A., & Pérez, J. (2018). Light as a limiting factor in microalgal cultivation: A review. *Renew. Sustain. Energy Rev.*, 81, 1–12.

Ma, S., Zeng, W., Huang, Y., Zhu, X., Xia, A., Zhu, X., & Liao, Q. (2022). Revealing the synergistic effects of cells, pigments, and light spectra on light transfer during microalgae growth: A comprehensive light attenuation model. *Bioresour. Technol.*, 348, 126777.

Ma, X.-N., Chen, T.-P., Yang, B., Liu, J., & Chen, F. (2016). Lipid production from *Nannochloropsis*. *Mar. Drugs*, 14, 61.

Miao, Y., Wang, X., Gao, L., Chen, Q., & Qu, M. (2016). Blue light is more essential than red light for maintaining the activities of photosystem II and I and photosynthetic electron transport capacity in cucumber leaves. *J. Integr. Agric.*, 15(1), 87–100.

Murata, N., Takahashi, S., Nishiyama, Y., & Allakhverdiev, S. I. (2012). Photoinhibition of photosystem II under environmental stress. *Biochim. Biophys. Acta - Bioenerg.*, 1817(1), 264–277.

Neelam, S., & Subramanyam, R. (2013). Alteration of photochemistry and protein degradation of photosystem II from *Chlamydomonas reinhardtii* under high salt grown cells. *J. Photochem. Photobiol. B Biol.*, 124, 63–70.

Núñez, M., & Quigg, A. (2016). Changes in growth and composition of the marine microalgae *Phaeodactylum tricornutum* and *Nannochloropsis salina* in response to changing sodium bicarbonate concentrations. *J. Appl. Phycol.*, 28, 2123–2138.

Nwoba, E. G., Parlevliet, D. A., Laird, D. W., Alameh, K., & Moheimani, N. R. (2019). Light management technologies for increasing algal photobioreactor efficiency. *Algal Res.*, 39, 101433.

Nzayisenga, J. C., Farge, X., Groll, S. L., & Sellstedt, A. (2020). Effects of light intensity on growth and lipid production in microalgae grown in wastewater. *Biotechnol. Biofuels*, 13, 1–8.

Posten, C. (2009). Design principles of photo-bioreactors for cultivation of microalgae. *Eng. Life Sci.*, 9(3), 165–177.

Pottier, L., Pruvost, J., Deremetz, J., Cornet, J. F., Legrand, J., & Dussap, C. G. (2005). A fully predictive model for one-dimensional light attenuation by *Chlamydomonas reinhardtii* in photobioreactors. *Biotechnol. Bioeng.*, 91(5), 569–582.

Quinn, J., Winter, L., & Bradley, T. (2011). Microalgae bulk growth model with application to industrial scale systems. *Bioresour. Technol.*, 102(8), 5083–5092.

Rao, M., Zou, X., Ye, J., Kuang, C., Chen, C., Huang, C., & Cheng, J. (2022). Light conditions determine optimal CO_2 concentrations for *Nannochloropsis oceanica* growth with carbon fixation. *ACS Sustain. Chem. Eng.*, 10(27), 8799–8814.

Richmond, A. (2004). Principles for attaining maximal microalgal productivity in photobioreactors: An overview. *Hydrobiologia*, 512, 33–37.

Richmond, A. (2013). Biological principles of mass cultivation. *Handbook of Microalgal Culture: Biotechnol. Appl. Phycol.*. pp. 171–204.

Rodolfi, L., Zittelli, G. C., Bassi, N., Padovani, G., Biondi, N., Bonini, G., & Tredici, M. R. (2009). Microalgae for oil: Strain selection, induction of lipid synthesis and outdoor mass cultivation in a low-cost photobioreactor. *Biotechnol. Bioeng.*, 102, 100–112.

Ruiz, J., Arbib, Z., Álvarez-Díaz, P. D., Garrido-Pérez, C., Barragán, J., & Perales, J. A. (2013). Photobiotreatment model (PhBT): A kinetic model for microalgae biomass growth and nutrient removal in wastewater. *Environ. Technol.*, 34, 979–991.

Schulze, P. S. C., Brindley, C., Fernandez, J. M., Rautenberger, R., Pereira, H., Wijffels, R. H., & Kiron, V. (2020). Flashing light does not improve photosynthetic performance and growth of green microalgae. *Bioresour. Technol. Rep.*, 100367.

Schulze, P. S., Barreira, L. A., Pereira, H. G., Perales, J. A., & Varela, J. C. (2014). Light emitting diodes (LEDs) applied to microalgal production. *Trends Biotechnol.*, 32, 422.

Schulze, P. S., Pereira, H. G., Santos, T. F., Schueler, L., Guerra, R., Barreira, L. A., Perales, J. A., & Varela, J. C. (2016). Effect of light quality supplied by light-emitting diodes (LEDs) on growth and biochemical profiles of *Nannochloropsis oculata* and *Tetraselmis chuii*. *Algal Res.*, 16, 387–398.

Sharma, Y., Chisti, Y., & Banerjee, U. C. (2020). Production, purification, characterization, and applications of lipases. *Biotechnol. Adv.*, 46, 107695.

Shetty, P., Gitau, M. M., & Maróti, G. (2019). Salinity stress responses and adaptation mechanisms in eukaryotic green microalgae. *Cells*, 8, 1657.

Short, A., Fay, T. P., Crisanto, T., Mangal, R., Niyogi, K. K., Limmer, D. T., & Fleming, G. R. (2023). Kinetics of the xanthophyll cycle and its role in photoprotective memory and response. *Nat. Commun.*, *14*(1).

Simionato, D., Sforza, E., Berges, J. A., & Dall'Osto, L. (2011). The response of *Nannochloropsis gaditana* to different types of light. *Bioresour. Technol.*, 102, 6026–6032.

Singh, V., & Mishra, V. (2022). A review on the current application of light-emitting diodes for microalgae cultivation and its fiscal analysis. *Crit. Rev. Biotechnol.*, *43*(5), 665–679.

Sirohi, R., Choi, H. I., & Sim, S. (2022). Microalgal fuels: Promising energy reserves for the future. *Fuel*, 312, 122841.

Solovchenko, A., Lukyanov, A., Solovchenko, O., Didi-Cohen, S., Boussiba, S., & Khozin-Goldberg, I. (2014). Interactive effects of salinity, high light, and nitrogen starvation on fatty acid and carotenoid profiles in *Nannochloropsis oceanica* CCALA 804. *Eur. J. Lipid Sci. Technol.*, 116(5), 635–644.

Spolaore, P., Joannis-Cassan, C., Duran, E., & Isambert, A. (2006). Commercial applications of microalgae. *J. Biosci. Bioeng., 101*(2), 87-96.

Sukenik, A., & Levy, R. (1993). Effect of light intensity and nutrient availability on the lipid production of the marine eustigmatophyte *Nannochloropsis sp. J. Phycol.*, 29(5), 670–676.

Tala, F., & Chow, F. (2014). Phenology and photosynthetic performance of *Porphyra* spp. (Bangiophyceae, Rhodophyta): Seasonal and latitudinal variation in Chile. *Aquat. Bot.*, 113, 107–116.

Thompson, G. A. (1996). Lipid and membrane function in green algae. *Biochim. Biophys*., 1302(1), 17–45.

Tyystjärvi, E. (2013). Photoinhibition of photosystem II. *Int. J. Mol. Sci.*, 14(7), 13713–13742.

Udayan, A., Pandey, A. K., Sirohi, R., et al. (2022). Production of microalgae with high lipid content and their potential as sources of nutraceuticals. *Phytochem. Rev.*, 22, 833–860.

Uyar, B., Ali, M. D., & Uyar, G. E. O. (2024). Design parameters comparison of bubble column, airlift and stirred tank photobioreactors for microalgae production. *Bioprocess Biosyst. Eng.*, 47, 195–209.

Verhulst, P.-F. (1838). Notice sur la loi que la population suit dans son accroissement. *Correspondance Math. Phys. Publ.*, 10, 113–121.

Vonshak, A., Novoplansky, N., Silva, A., Torzillo, G., Beardall, J., Palacios, Y., … & Palacios, Y. (2020). Photosynthetic characterization of two *Nannochloropsis* species and its relevance to outdoor cultivation. *J. Appl. Phycol.*, 32.

Walter, A., & Schöbel, H. (2023). Shed light on photosynthetic organisms: A physical perspective to correct light measurements. *Photosynth. Res.*, 156, 325–336.

Wu, S., Huang, A., Zhang, B., Li, H., Zhao, P., Lin, A., … & Wang, G. (2015). Enzyme activity highlights the importance of the oxidative pentose phosphate pathway in lipid accumulation and growth of *Phaeodactylum tricornutum* under CO_2 concentration. *Biotechnol. Biofuels*, 8(1).

Xin, X. G., Qian, G. Y., Chan, S. S., Xin, G. R., Chew, K. W., & Show, P. L. (2022). Current issues and challenges of applying microalgae in environmental biotechnology. *In* P. L. Show (Ed.), *Microalgae Environ. Biotechnol.* pp. 67-105.

Xu, H., Miao, X., & Wu, Q. (2017). Enhancing the lipid content of microalgae using different light wavelengths. *Algal Res.* 1, 21-30.

Yen et al. (2019): Yen, H.-W., Hu, I.-C., Chen, C.-Y., Nagarajan, D., & Chang, J.-S. (2018). Design of photobioreactors for algal cultivation. In A. Pandey, D.-J. Lee, Y. Chisti, & C. R. Soccol (Eds.), *Biofuels Algae*. pp. 225–256.

Young, A. J., & Britton, G. (1993). Carotenoids in photosynthesis. Chapman & Hall.

Zhou et al. (2020): Zhou, J., Yang, Y., Qiao, S., & Quan, X. (2020). Mitigating membrane fouling based on in situ •OH generation in a novel electro-Fenton membrane bioreactor. *Environ. Sci. Technol.*, 54(12), 7669–7676.

Zhu, B.-H., Sun, F.-Q., Yang, M., Lu, L., Yang, G.-P., & Pan, K.-H. (2014). Large-scale biodiesel production using flue gas from coal-fired power plants with *Nannochloropsis* microalgal biomass in open raceway ponds. *Bioresour. Technol.*, 174, 53–59.

Zhu, C. J., & Lee, Y. K. (1997). Determination of biomass dry weight of marine microalgae. *J. Appl. Phycol.*, 9, 189–194.

Annexes

Annex 1
Visual representations of light wavelengths combinations

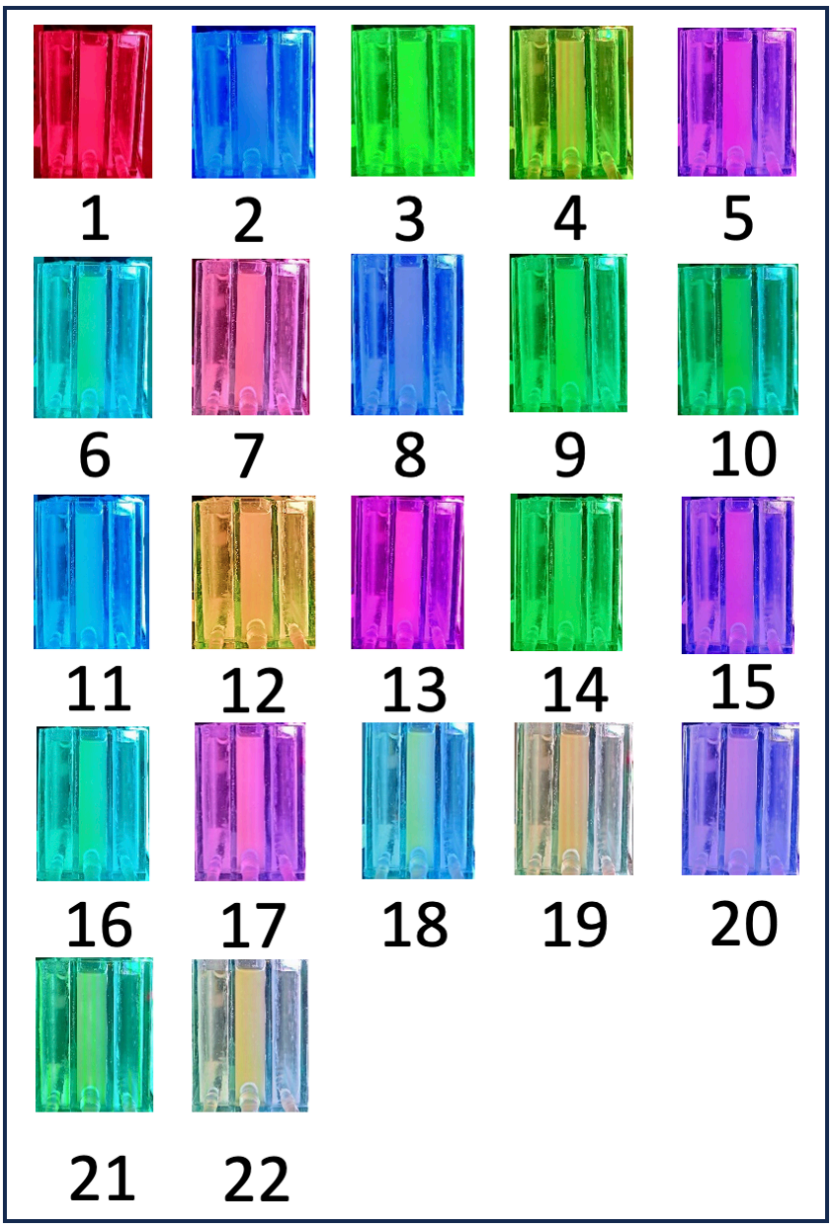

Figure A.1 - 1 Visual representation of the 22 light wavelength combinations previously described in Table 1 at 500 µmol m^{-2} s^{-1} in the photosynthetic chamber filled with *Phaeodactylum tricornutum* at 0.2 g L^{-1}

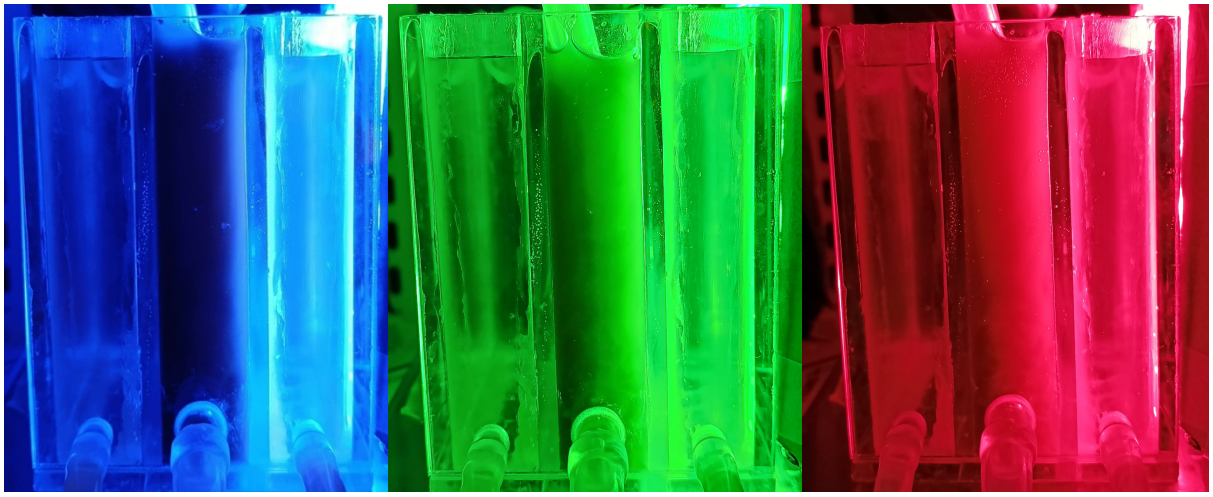

Figure A.1 - 2 Visual representation of dark-light zone ratios in the photosynthetic chamber under 500 µmol m^{-2} s^{-1} using blue (450nm), green (530nm) and red (620nm) with (a) *Phaeodactylum tricornutum* (2.0 g L^{-1}).

Annex 2
Predictive Models

Table A.2 - 1 Coordinates of all the tested light combinations on the ternary simplex centroid and respective photosynthetic oxygen evolution rates for each concentration (0.2, 2.0, and 5.0 g L^{-1}) and light intensity (500 and 1000 µmol m^{-2} s^{-1}).

Coordinates	Replicate	X1 (Red)	X2 (Green)	X3 (Blue)	r (*P. tricornutum* 2.0 g L^{-1} , 500 µmol m^{-2} s^{-1})POE(N.U.)	r(*P. tricornutum* 2.0 g L^{-1} , 1000 µmol m^{-2} s^{-1})POE(N.U.)	r(*P. tricornutum* 5.0 g L^{-1} , 500 µmol m^{-2} s^{-1})POE(N.U.)	r(*P. tricornutum* 5.0 g L^{-1} , 1000 µmol m^{-2} s^{-1})POE(N.U.)	r(*N. oceanica* 0.2 g L^{-1} , 500 µmol m^{-2} s^{-1})POE(N.U.)	r(*N. oceanica* 2.0 g L^{-1} , 500 µmol m^{-2} s^{-1})POE(N.U.)	r(*N. oceanica* 2.0 g L^{-1} , 1000 µmol m^{-2} s^{-1})POE(N.U.)	r(*N. oceanica* 5.0 g L^{-1} , 500 µmol m^{-2} s^{-1})POE(N.U.)	r(*N. oceanica* 5.0 g L^{-1} , 1000 µmol m^{-2} s^{-1})POE(N.U.)
e1	1	1	0	0	1.10	1.16	1.81	1.12	1.48	1.46	1.49	1.11	1.17
e2	1	0	0	1	0.44	0.59	-0.37	0.24	1.39	0.37	0.66	0.32	0.21
e3	1	0	1	0	0.87	0.96	0.74	0.78	0.86	0.70	0.96	0.85	0.79
e4	1	0.5	0.5	0	1.13	1.00	1.65	0.89	0.86	1.07	1.03	1.16	1.42
e5	1	0.5	0	0.5	1.04	0.88	0.91	0.89	1.1	1.04	0.98	0.91	1.09
e6	1	0	0.5	0.5	0.71	0.74	0.48	0.48	1.24	0.64	0.72	0.55	0.70
e7	1	0.8	0.1	0.1	1.41	1.17	1.76	0.99	1.32	1.21	1.02	1.27	1.16
e8	1	0.1	0.1	0.8	0.48	0.65	0.19	0.98	1.12	0.65	0.56	0.57	0.49
e9	1	0.1	0.8	0.1	0.71	0.43	0.89	0.72	0.96	0.88	1.06	0.78	0.93

e10	1	0.3(3)	0.3(3)	0.3(3)	0.93	1.01	1.04	0.07	0.81	0.87	1.05	0.74	0.92
e1	2	1	0	0	1.16	1.24	1.24	1.11	1.60	-	1.06	1.09	1.14
e2	2	0	0	1	0.47	0.39	-0.23	0.29	0.97	-	0.83	-0.17	0.18
e3	2	0	1	0	0.74	0.37	0.53	0.58	0.97	-	0.97	0.56	0.72
e4	2	0.5	0.5	0	0.99	0.47	1.06	0.87	1.36	-	1.23	1.31	1.22
e5	2	0.5	0	0.5	0.92	0.95	1.04	0.79	1.04	-	1.12	1.12	0.90
e6	2	0	0.5	0.5	0.56	0.78	0.49	0.57	1.11	-	0.86	0.14	1.24
e7	2	0.8	0.1	0.1	1.05	1.14	1.31	1.04	1.28	-	0.98	1.54	1.43
e8	2	0.1	0.1	0.8	0.52	0.84	0.39	0.50	1.26	-	0.81	-0.10	0.54
e9	2	0.1	0.8	0.1	0.85	1.02	0.84	0.72	1.14	-	0.98	0.29	1.20
e10	2	0.3(3)	0.3(3)	0.3(3)	0.89	-	0.83	0.88	1.09	-	1.04	0.73	1.12

Table A.2 - 2 Predictor models for *Phaeodactylum tricornutum* and *Nannochloropsis oceanica* for 3 concentrations (0.2, 2.0, and 5.0 g L^{-1}), 2 light intensities (500 and 1000 µmol m^{-2} s^{-1}), and their respective equation, *f*-value, *p*-value, R^2, predicted R^2, and the model's adequacy precision. X1, X2, and X3, represent red, green, and blue light ratios, respectively, as shown in Figure 11.

Model	Specie	Concentration ($g\ L^{-1}$)	Light Intensity ($\mu mol\ m^{-2\ -1}s$))	Mixture Order	Equation	F-value	p-value	R^2	Adj. R^2	Adeq. Prec.
MD1	*Phaeodactylum tricornutum*	2.0	500	Quadratic	$r = 1.16\ X_1 + 0.80\ X_2 + 0.43\ X_3 – 0.36\ X_1X_2 – 0.74\ X_1X_3 - 0.06\ X_2X_3$	44,41	< 0.001	0,91	0,90	17,82
MD2	*Phaeodactylum tricornutum*	2.0	1000	Linear	$r = 1.19\ X_1 + 0.66\ X_2 + 0.60\ X_3$	12,51	< 0.001	0,51	0,47	6,66
MD3	*Phaeodactylum tricornutum*	5.0	500	Quadratic	$r = 1.55\ X_1 + 0.65\ X_2 - 0.28\ X_3 + 1.01\ X_1X_2 + 1.40\ X_1X_3 + 1.21\ X_2X_3$	64,87	< 0.001	0,94	0,92	22,93
MD5	*Nannochloropsis oceanica*	0,2	500	Quadratic	$r = 1.54\ X_1 + 0.93\ X_2 + 1.20\ X_3 – 0.55\ X_1X_2 – 1.28\ X_1X_3 + 0.35\ X_2X_3$	7,57	< 0.001	0,64	0,56	8,55
MD6	*Nannochloropsis oceanica*	2.0	500	Quadratic	$r = 1.44\ X_1 + 0.74\ X_2 + 0.37\ X_3 – 0.08\ X_1X_2 + 0.34\ X_1X_3 + 0.37\ X_2X_3$	116,65	< 0.001	0,99	0,98	31,23
MD7	*Nannochloropsis oceanica*	2.0	1000	Linear	$r = 1.24\ X_1 + 0.98\ X_2 + 0.71\ X_3$	27,36	< 0.001	0,66	0,63	12,46
MD8	*Nannochloropsis oceanica*	5.0	500	Quadratic	$r = 1.17\ X_1 + 0.67\ X_2 + 0.064589\ X_3 + 1.17\ X_1X_2 + 1.49\ X_1X_3 - 0.60\ X_2X_3$	23,56	< 0.001	0,85	0,81	12,91
MD9	*Nannochloropsis oceanica*	5.0	1000	Quadratic	$r = 1.18\ X_1 + 0.78\ X_2 + 0.21\ X_3 + 1.30\ X_1X_2 + 0.98\ X_1X_3 + 1.65\ X_2X_3$	40,12	< 0.001	0,90	0,88	17,89

Annex 3

Dry Weight – Optical Density Correlation

Two scatter plots were created. One for *P. tricornutum* (Figure A.3 - 1) and another for *N. oceanica* (Figure A.3 - 2). The scatter plot illustrates the relation between the dry-weight biomass (g L^{-1}) of each microalga and the optical density measured at 750 nm. A linear regression was performed scoring a coefficient of determination of r^2=0.9732 and r^2=0.9858 for *P. tricornutum* (eq. 4) and *N. oceanica* (eq. 5), respectively.

$$DW\ (g\ L^{-1}) = 0.3418\ OD\ (750nm) \quad (4)$$

$$DW\ (g\ L^{-1}) = 0.2861\ OD\ (750nm) \quad (5)$$

These high r^2 values suggest that approximately 97.32% and 98.58%, respectively, of the variability in the dry-weight biomass can be explained by the optical density at 750 nm. These strong correlations implied that optical density at 750 nm was a reliable proxy for estimating the dry-weight biomass of the culture. These linear regressions were used to determine biomass concentration during the experimental trials.

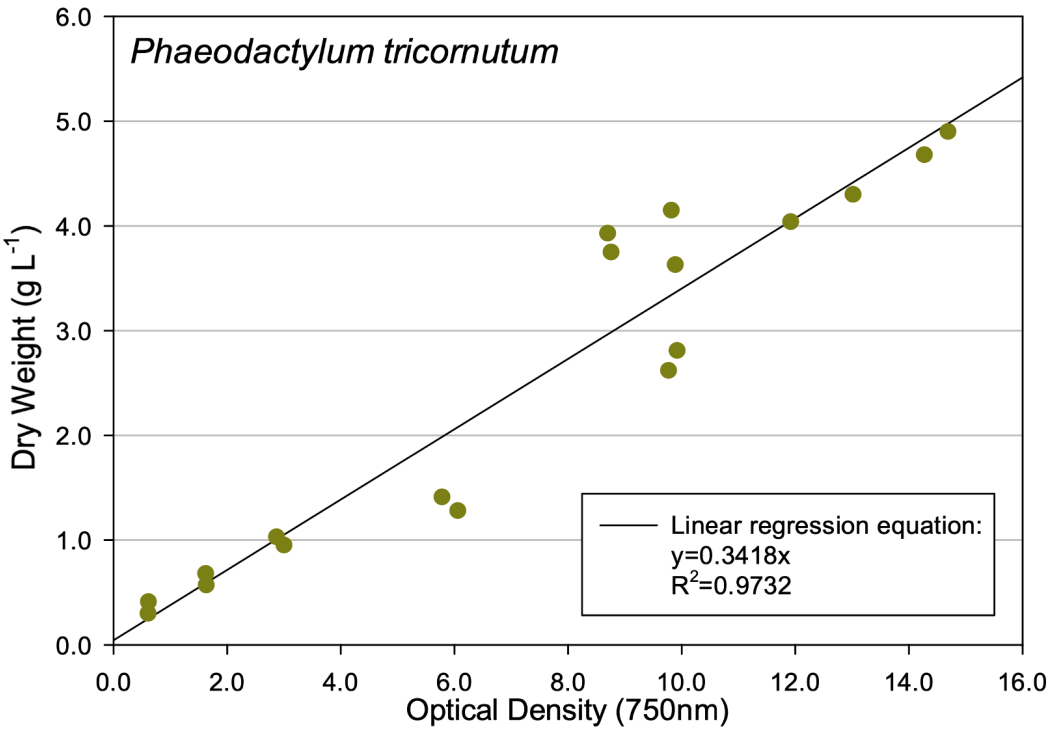

Figure A.3 - 1 Correlation between optical density (OD) and dry-weight (DW) measurements on *Phaeodactylum tricornutum*. The linear correlation equation: DW = 0.3418 OD and R^2=0.9732.

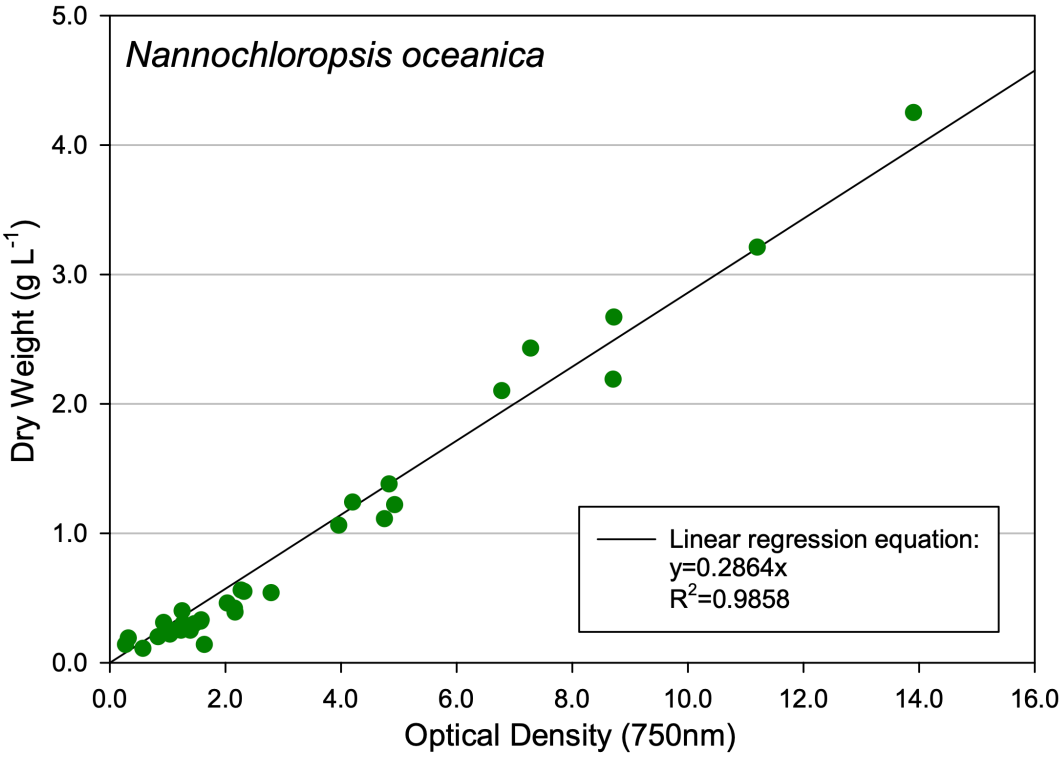

Figure A.3 - 2 Correlation between optical density (OD) and dry-weight (DW) measurements on *Nannochloropsis oceanica*. The linear correlation equation: DW = 0.2864 OD and R^2=0.9858.

Annex 4
AlgaeLum Prototype Development

AlgaeLum was a 3D-printed lamp designed to facilitate experiments on algae, specifically focusing on the effect of light quantity and quality. It counts with 2 developed iterations. The latter was used in the present study and counted with another experiment conducted by Arzum Gürsoy, supervised by Daniel Figueiredo from Associação Oceano Verde – GreenCoLab to investigate the effect of red (620 nm) and blue (450 nm) light quality on the concentration of fucoxanthin and chlorophyll *a* in *Phaeodactylum tricornutum*, and the effect of red and blue light quality on the concentration of chlorophyll *a* and *b* in *Tetraselmis chui* in GreenCoLab's facilities (Figure A.4 - 1).

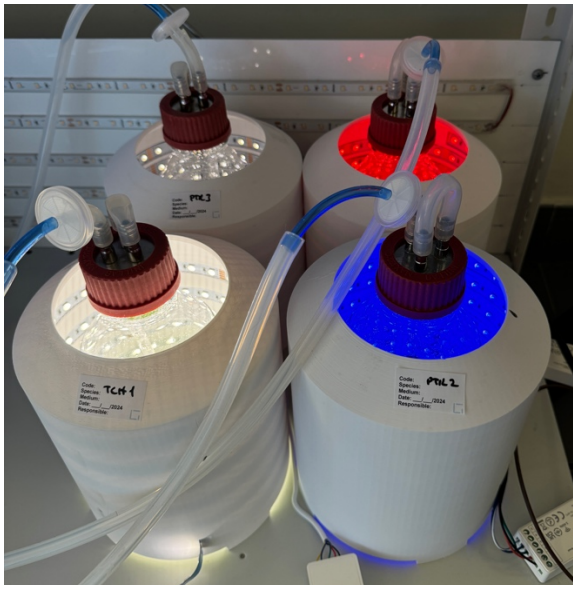

Figure A.4 - 1 Experiment to investigate the effect of blue and red light quality on the concentration evolution of specific pigments for *P. tricornutum* and *T. chui*, conducted in GreenCoLab's facilities by Arzum Gürsoy, supervised by Daniel Figueiredo.

<u>AlgaeLum version 0 – Conceptualization</u>

The conceptualization idea was tested with a flask (simulating a cultivation vessel) surrounded by an LED strip, due to their versatility in controlling light intensities and wavelengths (Figure A.4 - 2). This LED strip placement in a spiral around the dispenser would halve the light path because the light would be emitted from all angles around the vessel.

Figure A.4 - 2 AlgaeLum version 0 composed of a flask surrounded by an LED strip in a spiral.

AlgaeLum version 1

With the idea formulated, a 3D model of the first iteration was developed in Fusion360 software (Autodesk, San Rafael, CA, USA), and 3D printed in a Creality Ender 3 S1-Pro (Creality, Shenzhen, China) (Figure A.4 - 3). The spiral grooves were designed taking into consideration the length and the width of the 12V LED RGB strip used. The light intensity and wavelength could be controlled using a remote control with predefined light combinations from the LED manufacture.

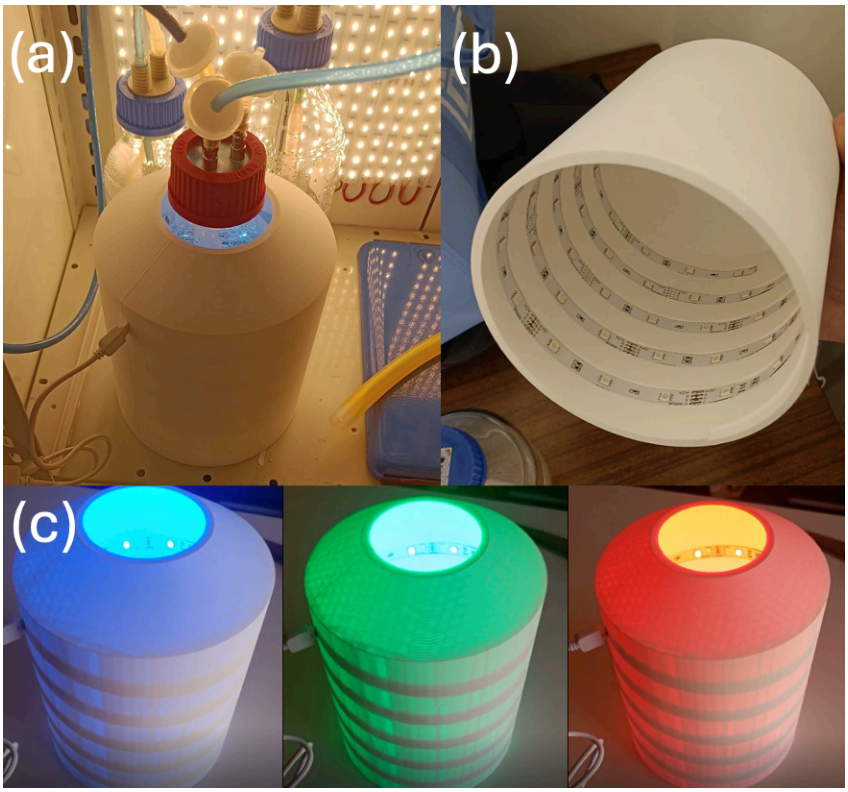

Figure A.4 - 3 (a) AlgaeLum v.1 first cultivation test. (b) AlgaLum v.1 RGB LED strip arrangement in a spiral. (c) AlgaeLum v.1 displaying blue, green, and red light, respectively.

AlgaeLum version 2

A new iteration was conceptualized, 3D modelled, 3D printed, and assembled (Figure A.4 - 4, Figure A.4 - 7 and Figure A.4 - 8). AlgaeLum version 2 featured a circular base embedded with a 24V fan in the center to allow airflow throughout the vessel in order to maintain room temperature. It used an LED RGBW controller, which was controlled via the MiBoxer mobile application (Figure A.4 - 5). This application allows users to manipulate the light intensities of the LEDs as well as the wavelengths emitted with over 6000 light combinations. The cylindrical base has a 10-degree slope, which ensures any spilled liquid flows away from the electronic components bay, and a central base socket to hold a 1L Schott flask along with a cylindrical acrylic spillage barrier to protect the LED strip. A cylindrical structure similar to AlgaeLum version 1 incorporates 4 meters of LED strip, illuminating the flask evenly. Regarding its light capabilities, white light (ranging between approximately 450 and 620 nm) could emit up to 1500 µmol m^{-2} s^{-1}, red (620 nm) up to 700 µmol m^{-2} s^{-1}, green (530 nm) and blue (450 nm) up to 1000 µmol m^{-2} s^{-1}, and altogether up to 2000 µmol m^{-2} s^{-1}.
The LED and fan were interconnected to an external quick connector, which was supplied with 24V through a 230V-24V transformer.

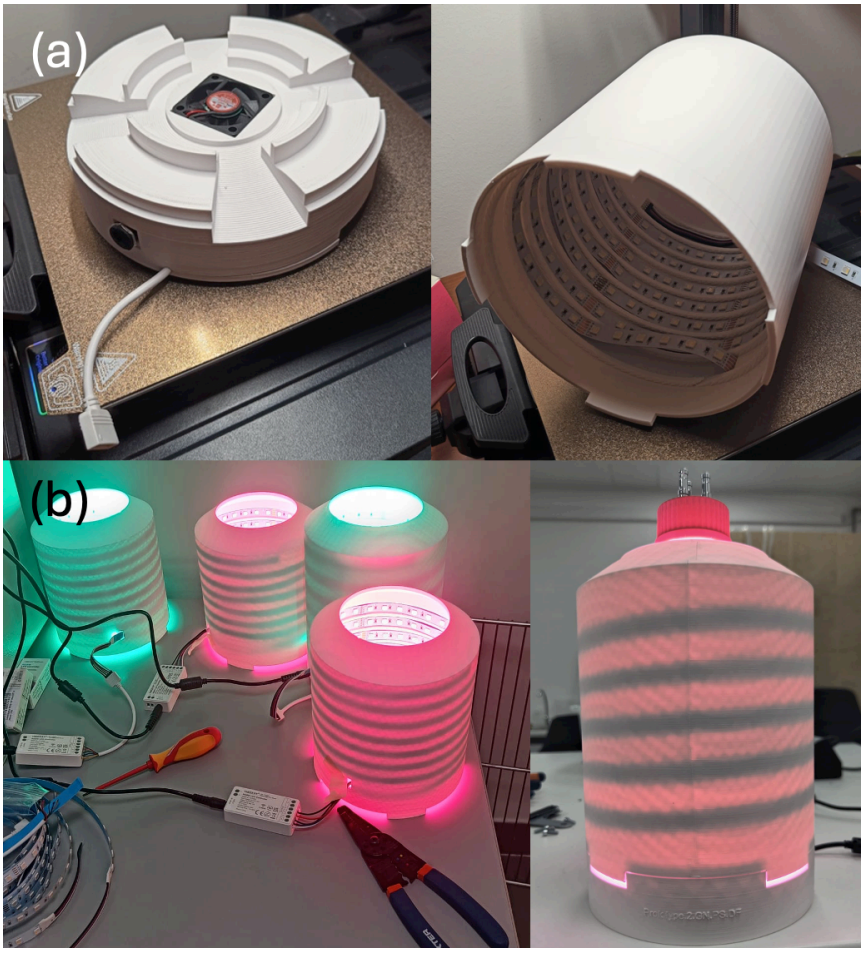

Figure A.4 - 4 (a) AlgaeLum v.2 base pos printed and assembled. (b) AlgaeLum v.2 displaying RGBW LED strips arrangement.

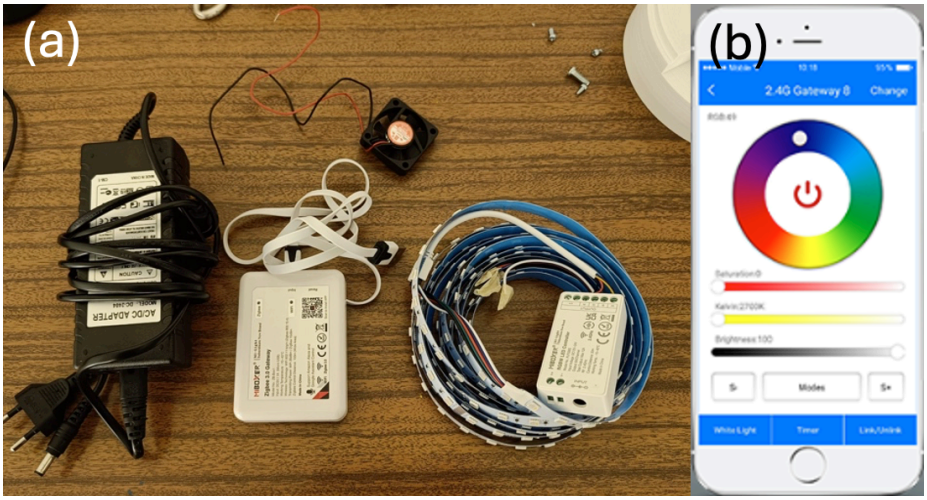

Figure A.4 - 5 (a) Hardware used in AlgaeLum v.2, 220V-24V power supply, MiBoxer gateway, Miboxer LED controller, 24v fan. (b) Visual representation of the MiBoxer application to control LEDs.

AlgaeLum lid

An additional accessory for the AlgaeLum version 2 was a custom-designed 3D-printed lid for the Schott flask (GL 32) made of autoclavable PP (polypropylene) equipped with ports for air, CO_2, a pH probe, and two inlets for a U-shaped aluminum water cooling tubing (Figure A.4 - 6). The implementation of customizable lids ensure control over variables such as pH, CO_2, culture volume, and temperature on the globally used Schott flask.

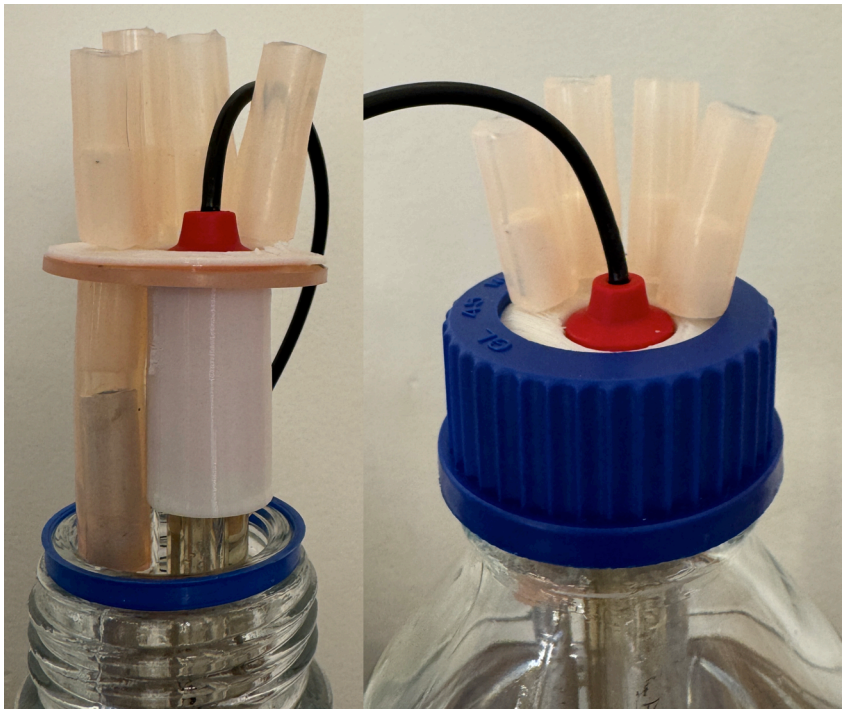

Figure A.4 - 6 AlgaeLum lid on a 1L Schott flask displaying an air outlet, an air inlet, a pH probe slot, and 2 inlets for water cooling tubing.

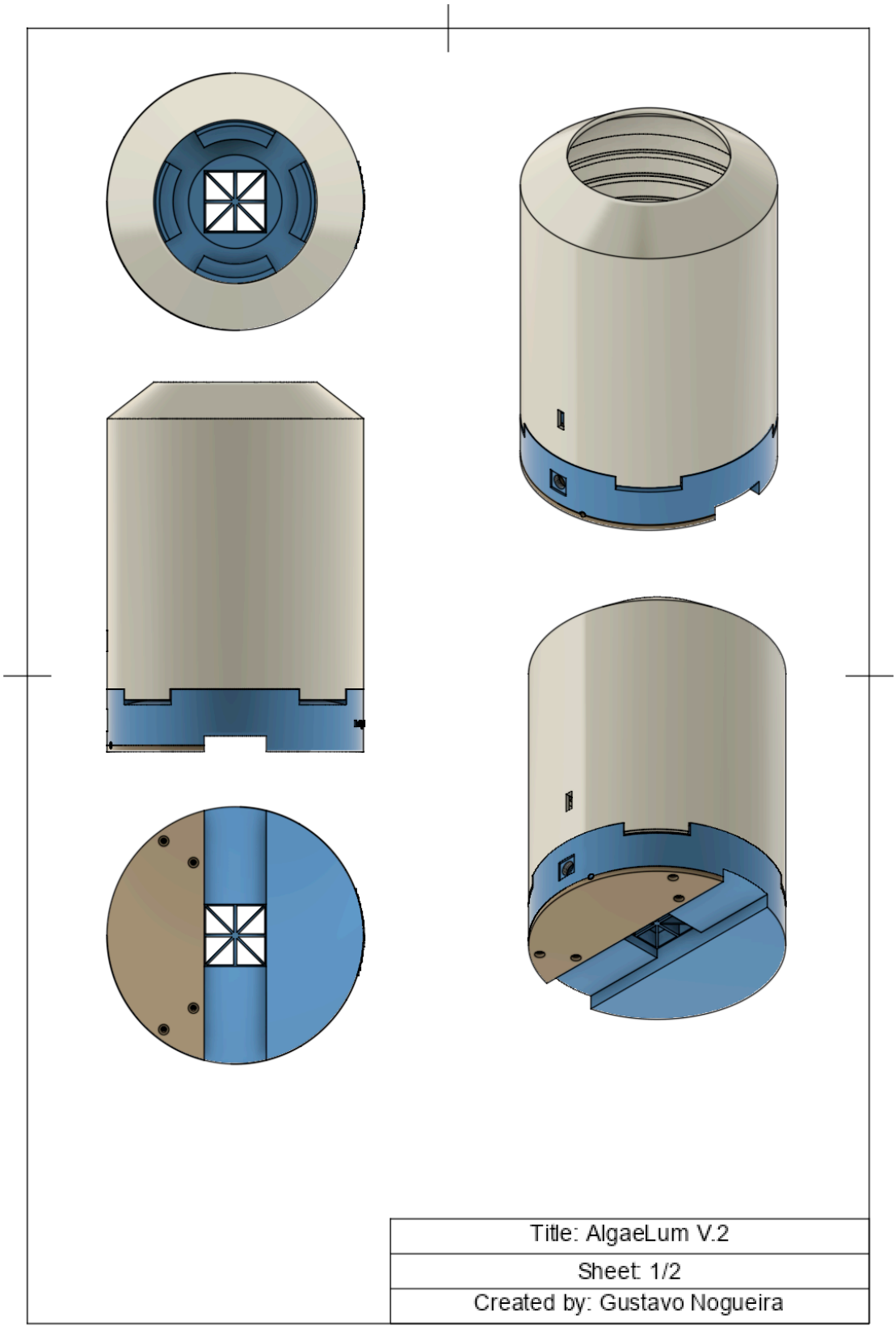

Figure A.4 - 7 AlgaeLum Version 2.0 conceptual technical drawing without dimensional details, focusing on the conceptual framework and component layout. Intended for visualization and ideation purposes (sheet 1/2).

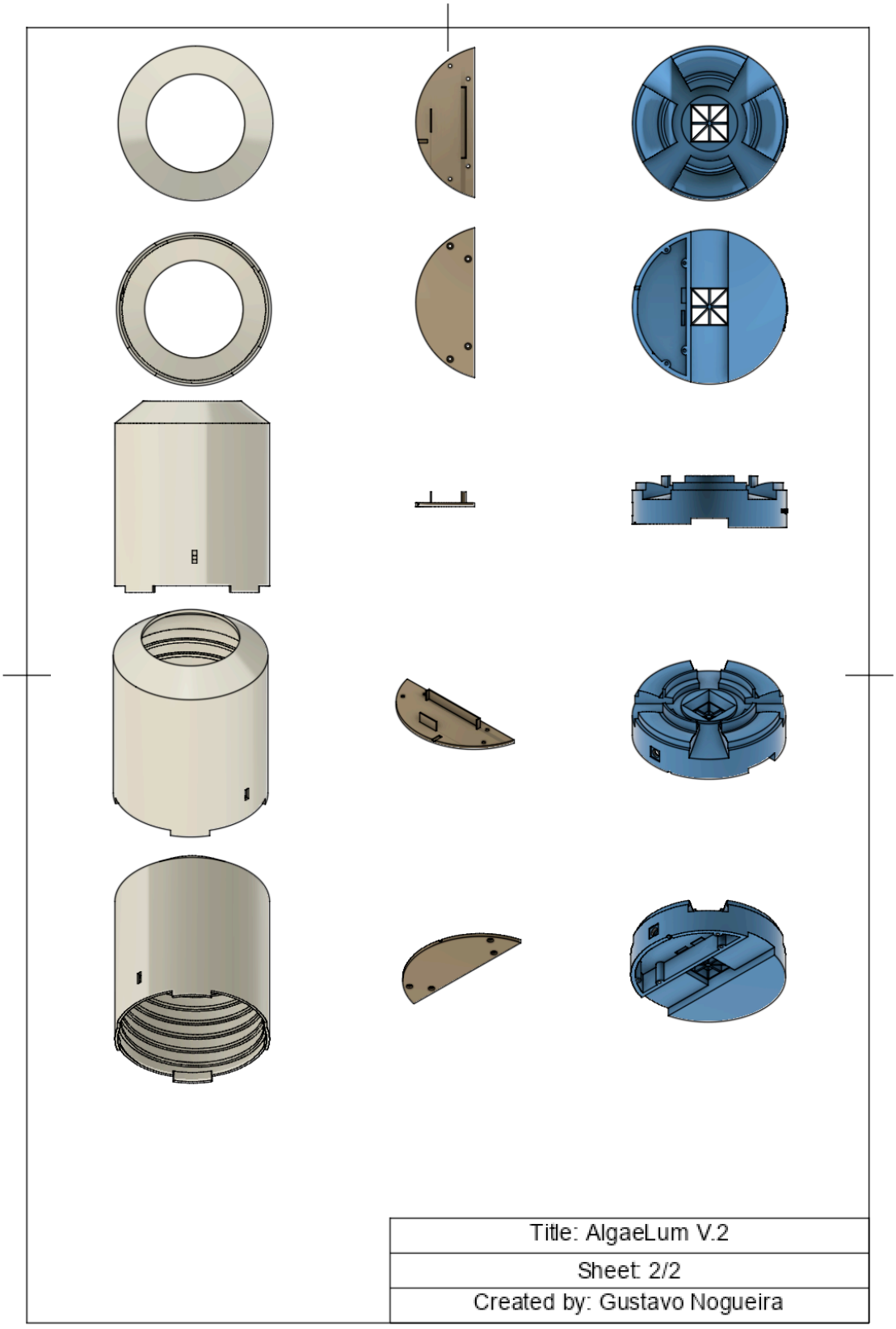

Figure A.4 - 8 AlgaeLum Version 2.0 conceptual technical drawing without dimensional details, focusing on the conceptual framework and component layout. Intended for visualization and ideation purposes (sheet 2/2).